

Sensitivity of Eigen Value to Damage and Its Identification

B.K.Raghuprasad¹, N.Lakshmanan², N.Gopalakrishnan², K.Muthumani²

Abstract: The reduction in natural frequencies, however small, of a civil engineering structure, is the first and the easiest method of estimating its impending damage. As a first level screening for health-monitoring, information on the frequency reduction of a few fundamental modes can be used to estimate the positions and the magnitude of damage in a smeared fashion. The paper presents the Eigen value sensitivity equations, derived from first-order perturbation technique, for typical infra-structural systems like a simply supported bridge girder, modelled as a beam, an end-bearing pile, modelled as an axial rod and a simply supported plate as a continuum dynamic system. A discrete structure, like a building frame is solved for damage using Eigen-sensitivity derived by a computational model. Lastly, neural network based damage identification is also demonstrated for a simply supported bridge beam, where the known-pairs of damage-frequency vector is used to train a neural network. The performance of these methods under the influence of measurement error is outlined. It is hoped that the developed method could be integrated in a typical infra-structural management program, such that magnitudes of damage and their positions can be obtained using acquired natural frequencies, synthesised from the excited/ambient vibration signatures.

Keywords: Eigen value sensitivity, Damage prediction, Structural health monitoring, Infra-structural system, Perturbation Analysis, Inverse Problem.

1 Introduction

A structural member can suffer varying degrees of damage due to reasons such as over loading, environmental ageing, corrosion, poor quality of construction, fatigue induced crack growth under cyclic loading, creep etc. Damage is an effect due to those causative factors and this manifest in the form of elongated and widened cracks, increased and residual deflections, loss of stiffness and increased time periods and damping. On many occasions it is required to take decisions regarding the repair and improvement of the damaged structure. The viability of repair has to be weighed with the cost of new replacement and this is governed by the state of damage suffered by the structure. Estimation of the magnitude of damage, location and its spread thus plays a crucial role in the repair methodology to be adopted. Also, residual strength and remaining life depends on the magnitude and position of damage. A structure is deemed to have been damaged if the structure, after un-loading could not return to its original state and there is a permanent deformation with loss of energy. Damage is defined, as per International Standards Organisation, as an unfavourable change in the condition of a structure that can affect the structural performance.

2 Damage Classifications

Damage indicators can be local or global. Localized damage indicators are better for giving a good picture of damage, whereas global indicators like frequencies, deflection etc are relatively less sensitive to local damage but are easier to measure. Also, it is seen that all the global damage indicators are essentially stiffness based. The problem in accurately defining damage essentially arises due to the fact that stiffness and strength are not linearly correlated. The stiffness and strength

¹ Indian Institute of science, Bangalore : 560012, India

² Structural Engineering Research Centre, CSIR campus, Taramani, Chennai: 600113, India

pair have definitely a correlation, but it is non-linear. At this stage it is also required to make a differentiation between concentrated damage and distributed damage. The damage undergone by a reinforced concrete bridge due to the effect of vehicle movement may be of distributed damage and a fatigue crack growth occurring on a steel plate may be a concentrated damage. For example in the case of a fatigue failure of a beam due to a central notch and subjected to cyclic loading, loss of stiffness (load per unit deflection) is minimal until just before the failure. It can be surmised that the correlation between the stiffness and damage is better for a distributed damage rather than for a concentrated damage.

Research in the area of damage detection and identification through changes in the fundamental frequencies and modal parameters of a structure saw a quantum jump during late eighties and early nineties. A comprehensive survey is presented by Doebling *et al.* (1996), who have reviewed the numerous technical literatures available on damage detection through vibration testing. Series of experiments and analytical predictions conducted by Swamidas and his colleagues and students hold a considerable bench-mark data for future researchers (Owolobi *et al.* (2003), Yang *et al.* (2001)). Lakshmanan *et al.* (1991), Rajagopalan *et al.* (1996, 1999) have correlated the cracking and yielding stiffness of the normal and fibre reinforced concrete beams, under various stages of pre-loading with the fundamental frequencies. A method is outlined such that from frequency measurements, maximum load carried by the bridge in its life time could be estimated. Hassiotis and Jeong (1993), Hassiotis (2000) outlines a method based on first order perturbation and optimization theory to compute the damage from measured natural frequencies.

Identification of damage locations in plate-like structures using strain modal approach is proposed by Li, *et al.* (2002), using bending moment index and residual strain mode shape index. A combined static and dynamic approach for damage identification using curvature mode shape and strain frequency response function is proposed by Yam *et al.* (2002). Perturbation theory enhanced

finite element method is used to train the artificial neural network, using damage response towards identification by Yu *et al.* (2007). A damage identification theory, based on continuum damage mechanics and the damage modelled as effective orthotropic elastic stiffness is formulated and verified from the forced vibration response of a damaged plate. (Lee *et al.* (2003)). Non-linear elastic wave spectroscopy is used for the damage identification of composite plates by Meo and Zumpano (2005). Sensitivity of orthogonality conditions of the mode shapes is used by Santos, *et al.* (2000) for the damage identification of composite plates. An equation error approach is developed and tested for a coupled beam and plate system by Roy *et al.* (2006). Damage identification of plate structures using changes in modal compliances is proposed by Choi *et al.* (2005). Frequency shifts for the first few fundamental modes is used to generate the Fourier coefficients of stiffness variation caused by damage, in a rod and beam element by Morassi (2007). A statistical damage identification algorithm based on perturbation method with a two stage model updating is used in damage detection in the presence of Gaussian noise by Xia and Hao (2003). A residual-force concept in conjunction with matrix condensation approach is used in the damage identification of a cantilever and a ten-storied steel frame by Ge and Lui (2005). Spatial wavelet transforms are used to identify the damages in a rod subjected to forced vibrations by Castro *et al.* (2000). Global structural force-deformation response and averaged local experimental information is used to create a well-conditioned inverse problem for damage identification by Iacono *et al.* (2006). Liu and Yang (2006) propose a novel three-step (number of damaged elements, localising and quantification) approach for damage identification, validated by a planar truss. The system matrices of a frame element are decomposed into their static eigen values and vectors and their inspection is used to derive the damages by Wu Di and Law (2007).

3 Effect of Damage on the Natural Frequencies

In the study damage is modeled as a reduction in the flexural rigidity (EI or D or AE) of a few elements. (Fig. 1 to Fig. 3). α is taken as the ratio of the reduced EI to original EI. The location of damage is the position of the center of damage from one end of the beam (l_0). This is normalized with reference to the span of the beam (l). Similarly extent of damage ($2b_0$) is also normalized with reference to the length. The parameters that control the natural frequencies of the simply supported beam with a single damage location is given as,

$$f_{n,d} = F(l_0, 2b_0, l, E, I, \rho, A, \alpha) \quad (1)$$

where, $f_{n,d}$ is the damaged frequency of the beam at the 'n-th' mode. l = Span of the Beam. l_0 = Location of Centre of Damage. $2b_0$ = Extent of length of damage EI = Flexural Rigidity of Beam. A = Area of Beam. ρ = Mass Density of the Beam. α = Ratio of reduced EI to the original un-damaged EI.

After suitably grouping the parameters into non-dimensional form, it is possible to write the equation as,

$$\delta_n = 1 - \left(\frac{f_{n,d}}{f_{n,ud}} \right)^2 = F_1\left(\frac{l_0}{l}, \frac{2b_0}{l}, \beta\right) \quad (2)$$

where, $\beta = (1 - \alpha)$.

In the case of a plate, the equation is written as,

$$\delta_n = 1 - \left(\frac{f_{n,d}}{f_{n,ud}} \right)^2 = F_2\left(\frac{l_{0x}}{l}, \frac{l_{0y}}{l}, \frac{2b_{0x}}{l}, \frac{2b_{0y}}{l}, \beta\right) \quad (3)$$

∞ = Ratio of reduced flexural rigidity D_d to the original un-damaged D.

$$D = \frac{E \cdot t^3}{12(1 - \mu^2)} \quad (4)$$

The parameters in the above equation used for defining the damage for a simply supported plate structure is as follows: l_x, l_y = Span of the plate in X and Y directions. l_{0x}, l_{0y} = Location of Centre of Damage in X and Y directions. $2b_{0x}, 2b_{0y}$

= Extent of damage in X and Y-directions. D = Flexural Rigidity of plate. M = Total mass of the plate. ρ = Mass Density of the plate. β = magnitude of damage. n, m = mode numbers in x and y-direction. f = natural frequency in cycle/sec.

In the case of an axial rod,

$$\delta_n = 1 - \left(\frac{f_{n,d}}{f_{n,ud}} \right)^2 = F_1\left(\frac{l_0}{l}, \frac{2b_0}{l}, \beta\right) \quad (5)$$

∞ = Ratio of reduced AE to the original un-damaged AE.

It is seen from the above equation that the change in the ratio of the damaged and undamaged Eigen values (square of natural frequencies), which constitute the RHS of equations is a function of the normalized position of damage, $\frac{l_0}{l}$, normalized extent of damage $\frac{2b_0}{l}$ and the change in the ratio of damaged EI (D or AE) with reference to the original EI (β). It is seen that, if the LHS is zero, no damage has occurred to the system, which also implies that $\beta = 0$. Similarly, if LHS is 1.0, damage is full and $\beta = 1$. $1 - \left(\frac{f_{n,d}}{f_{n,ud}} \right)^2$ is analogous to the global damage and β is analogous to the local damage.

4 Estimation of natural frequency reduction for a known damage

For the condition of a damaged structure, wherein the mass matrix does not undergo any change from the original matrix, it is possible to derive the equation for the changed Eigen values and vectors from the first-order perturbation technique :

$$\begin{aligned} \lambda_i &= \lambda_i^{(0)} + p_i^{(0)T} K_1 p_i^{(0)} \\ p_i &= p_i^{(0)} + \sum_{\substack{r=1 \\ r \neq i}}^n \left(\frac{p_r^{(0)T} K_1 p_i^{(0)}}{\lambda_i^{(0)} - \lambda_r^{(0)}} \right) \cdot p_r^{(0)} \end{aligned} \quad (6)$$

$\lambda_i, \lambda_i^{(0)}$: Post and Pre damage i-th Eigen values, $p_i, p_i^{(0)}$: Post and Pre damage i-th Eigen vectors, K_1 : Perturbation content of the stiffness matrix (Sparse).

From the above expressions, it can be noted that only the i^{th} un-perturbed parameters enter into the

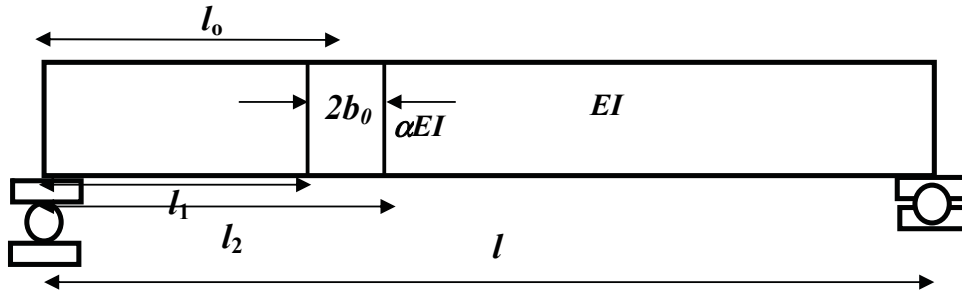


Figure 1: A Simply Supported Beam with a reduced EI for portion of its length

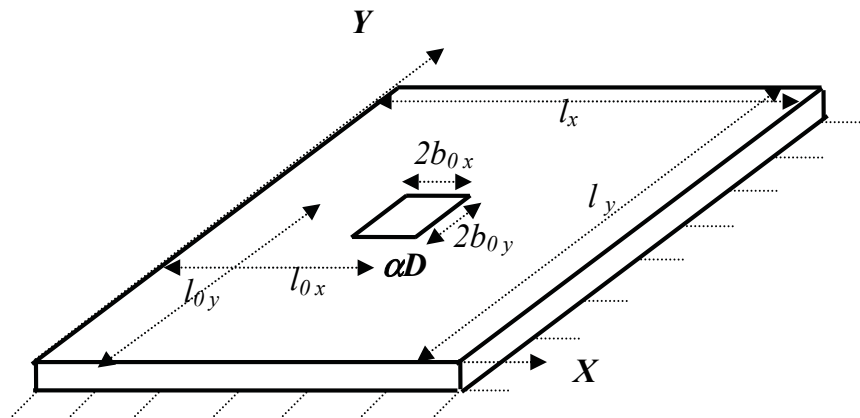


Figure 2: A thin rectangular simply supported plate with a Discrete Defect

calculations of perturbed Eigen values, whereas the complete un-perturbed Eigen solution is required for the computation of perturbed Eigen vectors. The insights from the above equation is that : *The change in Eigen value due to a damage is equivalent to twice the strain energy release in the damaged zone, under the action of an ortho-normalised displacement profile.*

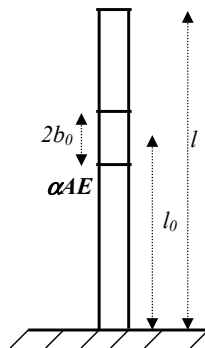


Figure 3: An Axial Bar Element Supported at One End, with a Discrete Defect

5 Simply supported Beam

5.1 Forward Problem

For a continuous system, the matrix equation, mentioned earlier can be modified as,

$$\Delta\omega^2 = \frac{\int_{l_0-b_0}^{l_0+b_0} \beta \cdot EI \cdot \left(\frac{\partial^2 y}{\partial x^2}\right)^2 dx}{\int_0^l \bar{m} y^2 dx} \tag{7}$$

where $y_n(x) = \sin\left(\frac{\pi n x}{l}\right)$ is the mode shape corresponding to the un-damaged state. Simplifying, the following expression for the normalized natural frequency is obtained for the damaged simply supported beam.

$$\left(\frac{\omega_d}{\omega_{ud}}\right)_n = \sqrt{1 - 2\beta \left[\frac{b_0}{l} - \frac{1}{2n\pi} \left(\cos \frac{2n\pi l_0}{l} \cdot \sin \frac{2n\pi b_0}{l} \right) \right]} \tag{8}$$

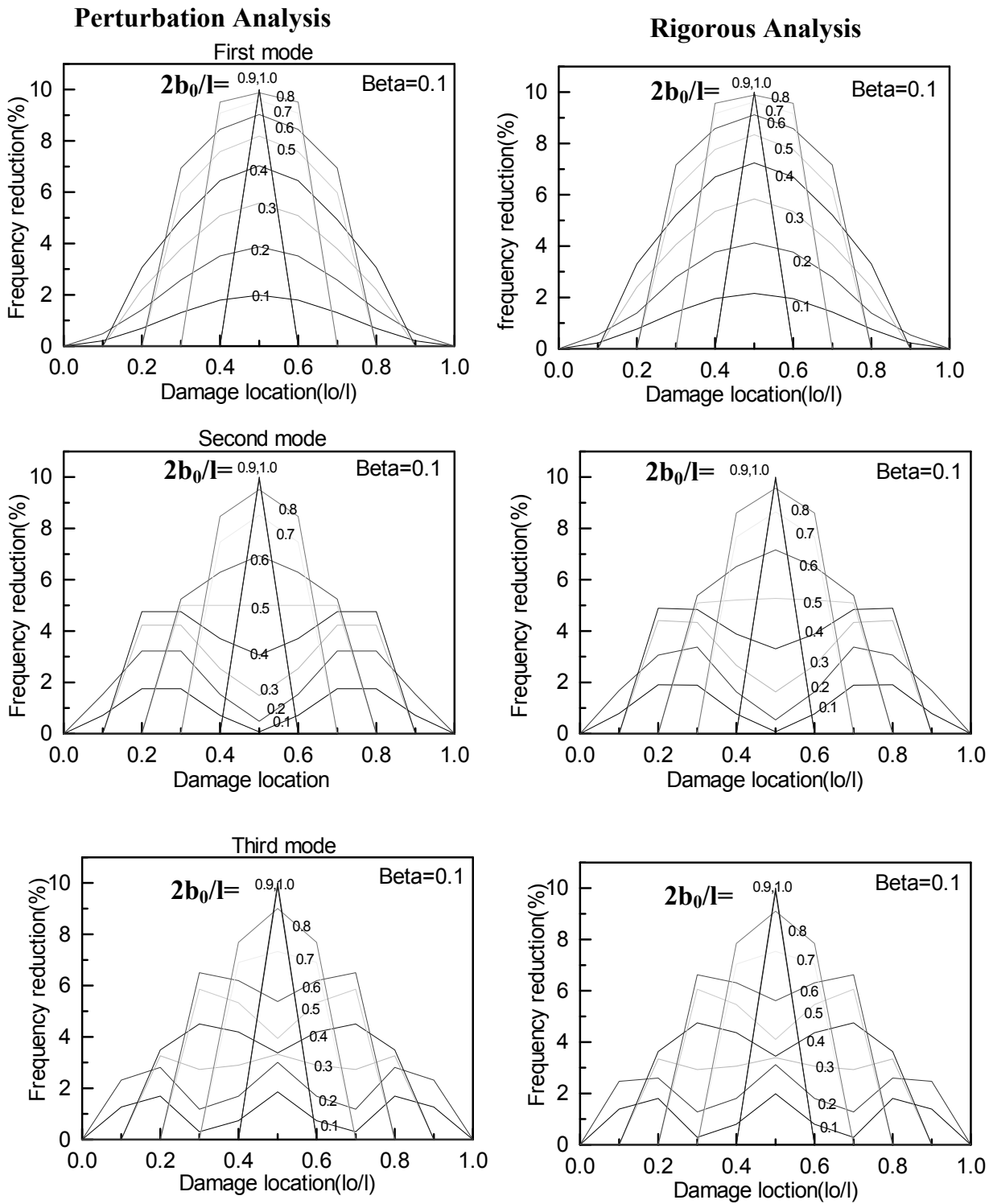


Figure 4: Comparison of Perturbation Analysis with Rigorous Analysis (Beta = 0.1)

Fig-4 shows a comparison of δ_n as predicted by the perturbation equation derived above, vis-à-vis the actual values, for $\beta=0.1$. From similar figures, drawn for higher β values, (not given in this paper), It can be noticed that up to 25% damage, both the results are identical. Between 25% to 30% tolerable deviation is seen. But for 40% damage and above, the perturbation values are less than rigorous analysis values. Hence it can be concluded that the first order perturbation equation is valid up to 30% damage.

5.2 Simply supported Beam – Inverse Problem

Inverse problem is the one in which the measured frequencies and mode shapes are used to compute the damage magnitude and the position of damage. As frequencies of a bridge can be measured, with relative ease, a method is developed such that damage could be predicted from the changes in measured frequencies alone.

For a multiple damage scenario, Equation – 8 in is modified and written as,

$$1 - \left(\frac{\omega_d}{\omega_{ud}} \right)_n^2 = \sum \beta_j \left[\frac{2b_{0,j}}{\ell} - \frac{1}{n\pi} \left(\cos \frac{2n\pi l_{0,j}}{\ell} \cdot \sin \frac{2n\pi b_{0,j}}{\ell} \right) \right] \quad (9)$$

In the above equation, β_j is the reduction in EI at the 'j-th' segment and the damage exists for a length of $2b_{0,j}$ and the distance to the mid-point of this segment is $l_{0,j}$. An equation like this can be written for each measured frequency and there will be 'n' equations corresponding to 'n' measured frequencies. The above equation can be written in a matrix form in the following manner and the information of damage could then be obtained for as many locations as the number of measured frequencies.

$$\{\varepsilon\} = [A] \{\beta\} \quad (10)$$

$$\varepsilon_i = 1 - \left(\frac{\omega_d}{\omega} \right)_i^2 \quad (11)$$

$$A_{ij} = \frac{2b_{0,j}}{l} - \frac{1}{i\pi} \left(\cos \frac{2i\pi l_{0,j}}{l} \cdot \sin \frac{2i\pi b_{0,j}}{l} \right)$$

In the above equation 'i' is the variation for the number of measured modes and 'j' is the variation of number of beam segments. **A** is the Eigen sensitivity matrix.

Towards validating the above procedure, a numerical exercise is carried out for a simply supported beam, in which damage is introduced in the form of reduced EI at ten equal segments (0.1l). Natural frequencies for the first five modes are computed during the un-damaged state of the beam and after inducing damage. This gives rise to LHS of Equation (10), where the ratio of the change in the Eigen values after occurrence of damage to the original Eigen value is to be given. The sensitivity matrix [A] is a function of the length and mid-positions of segments. Using the information and making use of symmetry, total numbers of unknowns are five and to evaluate these unknowns, five equations are available. A program is written, which takes the frequencies of the beam before and after damage. Using this input, the program computes the damage on each of the beam segment. The damage distribution is assumed as symmetric.

Fig-5 shows the comparison of damages predicted by the method vis-à-vis the actual damages. As can be seen from these figures, a wide variation of damage patterns are given and tested to evaluate the efficiency of the developed method. It is summarized that as in the forward problem, the inverse problem using perturbation analysis is able to predict the damages well up to 40% of local damage.

6 Simply supported Plate

6.1 Forward Problem

Strain energy function of the plate (Eqn. 12) and its mode shapes are made use to derive the changes in Eigen values of a simply supported

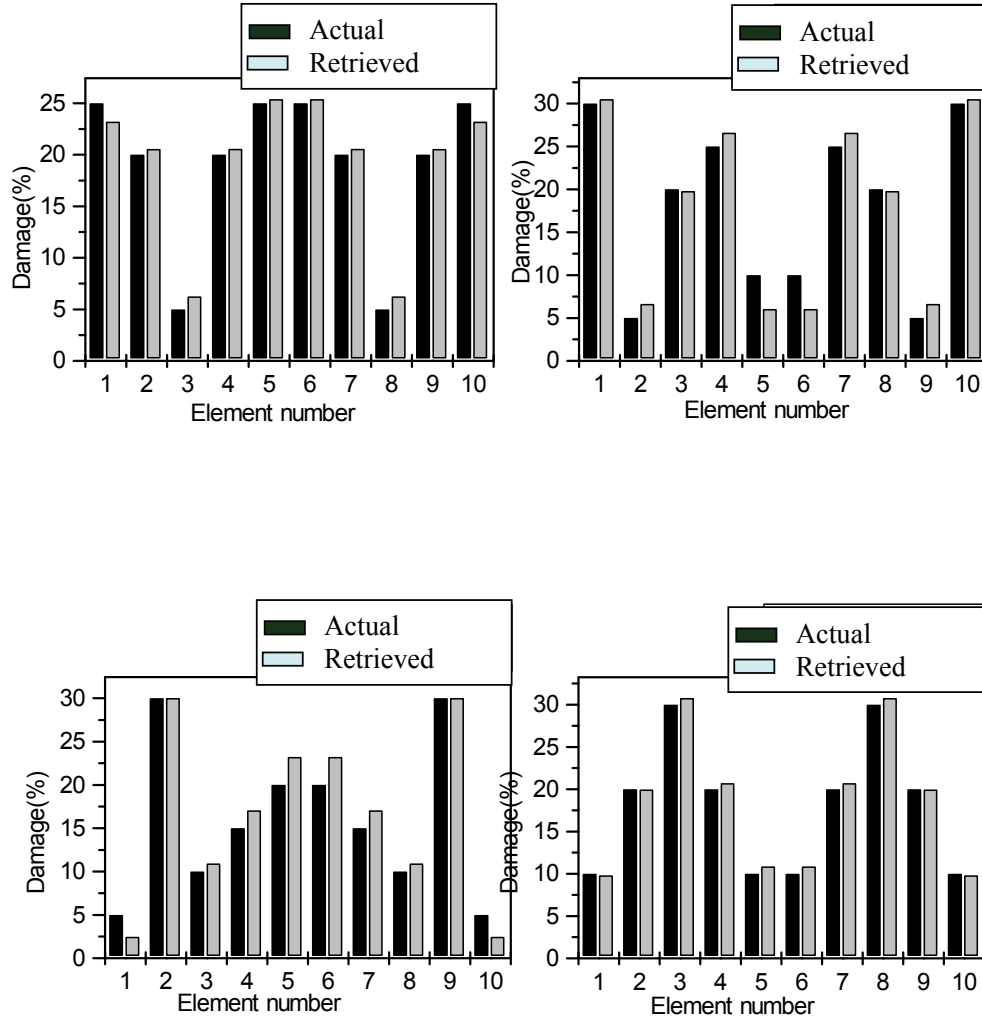


Figure 5: Comparison of Damage Predicted by Perturbation Analysis with Actual Damage Values

thin plate

$$U = \frac{D}{2} \int \left\{ \left(\frac{\partial^2 \omega}{\partial x^2} + \frac{\partial^2 \omega}{\partial y^2} \right)^2 - 2(1-\mu) \left[\frac{\partial^2 \omega}{\partial x^2} \cdot \frac{\partial^2 \omega}{\partial y^2} - \left(\frac{\partial^2 \omega}{\partial x \partial y} \right)^2 \right] \right\} dx dy \quad (12)$$

where, the mode shape corresponding to undamaged state is $\omega_n(x, y) = \sin \frac{n\pi x}{\ell} \cdot \sin \frac{m\pi y}{\ell}$. For a single damage case, Eigen value change is

written as,

$$\Delta f^2 = \frac{\beta \cdot D}{0.25M} \left\{ \left[\frac{n^2 \pi^2}{\ell_x^2} + \frac{m^2 \pi^2}{\ell_y^2} \right]^2 C_1 + \left[4(1-\mu) \frac{n^2 m^2 \pi^4}{\ell_x^2 \cdot \ell_y^2} \right] C_2 \right\} \quad (13)$$

The C_1 and C_2 are given as,

$$C_1 = \left[b_{ox} - \frac{\ell_x}{2n\pi} \left(\sin \frac{2n\pi b_{ox}}{\ell_x} \cos \frac{2n\pi \ell_{ox}}{\ell_x} \right) \right] \times \left[b_{oy} - \frac{\ell_y}{2m\pi} \left(\sin \frac{2m\pi b_{oy}}{\ell_y} \cos \frac{2m\pi \ell_{oy}}{\ell_y} \right) \right]$$

$$C_2 = \left[b_{ox} \cdot \frac{\ell_y}{2m\pi} \sin \frac{2m\pi b_{oy}}{\ell_y} \cos \frac{2m\pi \ell_{oy}}{\ell_y} \right] + \left[b_{oy} \cdot \frac{\ell_x}{2n\pi} \sin \frac{2n\pi b_{ox}}{\ell_x} \cos \frac{2n\pi \ell_{ox}}{\ell_x} \right] \quad (14)$$

Flexural Rigidity D is, $D = \frac{E \cdot t^3}{12(1-\mu^2)}$.

For the case of a widespread, uniform reduction in 'D', substituting, $b_{oy} = l_{oy} = l_y/2$; $b_{ox} = l_{ox} = l_x/2$; Equation for Eigen-value reduction is

$$\Delta f^2 = \frac{\beta \cdot D}{0.25M} \left[\frac{n^2 \pi^2}{\ell_x^2} + \frac{m^2 \pi^2}{\ell_y^2} \right]^2 \frac{\ell_x \ell_y}{4} \quad (15)$$

The equation can be easily verified.

Validity of Equations – 13 & 14 is verified using a finite element analysis (ANSYS -5.4) conducted on a 6 m (x) × 4 m (y) X 50 mm simply supported steel plate. The plate is subjected to quarter symmetric damage profiles with six divisions in X-axis and four divisions in Y-axis. The position of damage segments are shown in Fig. 6. $\beta_1, \beta_2, \beta_3$ are the damages along the X-edge and β_1, β_4 are along Y-edge and β_5, β_6 are the interior values. Six damage profiles are used in both forward and inverse analysis. They are

Case-1: $\{\beta\} = \{ 0.20; 0.05; 0.20; 0.05; 0.20; 0.05 \}$

Case-2: $\{\beta\} = \{ 0.10; 0.15; 0.17; 0.15; 0.20; 0.25 \}$

Case-3: $\{\beta\} = \{ 0.20; 0.10; 0.15; 0.10; 0.25; 0.30 \}$

Case-4: $\{\beta\} = \{ 0.25; 0.15; 0.20; 0.20; 0.30; 0.40 \}$

Case-5: $\{\beta\} = \{ 0.30; 0.10; 0.25; 0.15; 0.40; 0.50 \}$

Case-6: $\{\beta\} = \{ 0.20; 0.25; 0.50; 0.30; 0.40; 0.60 \}$

Using Eqn. (13, 14) and further making use of Eqns. (16) and (17), the frequencies of the plate after damage are computed using ANSYS and the

comparison with perturbation equation is shown in Tables -1 and -2.

$$f_{n,m} = \pi^2 \left[\left(\frac{n}{\ell_x} \right)^2 + \left(\frac{m}{\ell_y} \right)^2 \right] \sqrt{\frac{D}{m}} \quad (16)$$

$$f_d^2 = f_{ud}^2 - \Delta f_d^2 \quad (17)$$

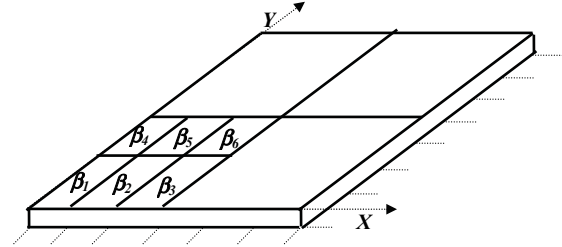


Figure 6: A thin rectangular simply supported plate with number of Damage Locations

6.2 Simply supported Plate – Inverse Problem

An equation like (10) can be written for each measured frequency and there will be 'n' equations corresponding to 'n' measured sets of frequencies. The Equation (10) can be written in a matrix form in the following manner and the information of damage could then be obtained for as many locations as the number of measured frequencies.

$$\{\varepsilon\} = [A] \{\beta\} \quad \varepsilon_i = 1 - \left(\frac{f_d}{f_{ud}} \right)_i^2 = \Delta f_d^2 \quad (18)$$

Re-generated damage values are:

Case-1: $\{\beta\} = \{ 0.210; 0.054; 0.216; 0.061; 0.194; 0.050 \}$

Case-2: $\{\beta\} = \{ 0.102; 0.155; 0.179; 0.159; 0.196; 0.249 \}$

Case-3: $\{\beta\} = \{ 0.187; 0.115; 0.167; 0.118; 0.249; 0.303 \}$

Case-4: $\{\beta\} = \{ 0.285; 0.151; 0.251; 0.214; 0.272; 0.401 \}$

Case-5: $\{\beta\} = \{ 0.360; 0.110; 0.350; 0.200; 0.350; 0.490 \}$

Table 1: Comparison of Frequencies for Plate after damage

Set no:	n	m	Natural frequency(f_d) For case-1		Natural frequency(f_d) For case-2		Natural frequency(f_d) For case-3	
			Perturbation	FEM	Perturbation	FEM	Perturbation	FEM
1	1	1	10.167	10.147	9.748	9.7394	9.551	9.5294
2	2	1	19.251	19.202	18.903	18.881	18.621	18.568
3	1	2	31.171	31.071	30.037	29.975	29.828	29.674
4	3	1	35.243	35.144	33.937	33.875	33.635	33.495
5	2	2	40.523	40.400	39.447	39.375	39.182	39.021
6	3	2	56.109	55.900	54.647	54.528	54.206	53.985

Table 2: Comparison of Frequencies of Plate after Damage

Set no:	n	M	Natural frequency(f_d) For case-4		Natural frequency(f_d) For case-5		Natural frequency(f_d) For case-6	
			Perturbation	FEM	Perturbation	FEM	Perturbation	FEM
1	1	1	9.105	9.0691	8.716	8.6345	8.224	8.1234
2	2	1	17.865	17.799	17.232	17.045	16.330	16.065
3	1	2	28.560	28.312	27.595	27.028	25.007	24.491
4	3	1	32.084	31.941	31.214	30.780	29.147	28.770
5	2	2	37.621	37.418	36.816	36.261	34.476	33.829
6	3	2	51.946	51.515	50.779	49.711	47.420	45.828

Case-6: $\{\beta\} = \{ 0.436; 0.220; 0.640; 0.340; 0.300; 0.560 \}$

Figs 7.1 to 7.4 show the actual damage bar graphs (Left) compared with predicted values (Right) for case-1 to case-4).

7 Axial Rod Element

7.1 Forward Problem

The strain energy equation for axial element is given by,

$$U = \frac{1}{2} \int_0^{\ell} AE \left(\frac{\partial u}{\partial x} \right)^2 \cdot dx \quad (19)$$

where, the mode shape is $u_{(x)} = \sin(2k-1) \frac{\pi x}{2\ell}$ and corresponding to the initial un-damaged state. The natural frequency for undamaged axial structural element is given by,

$$f_{ud} = (2k-1) \frac{\pi}{2} \sqrt{\frac{EA}{M\ell}} \quad (20)$$

The reduction in Eigen values can be obtained as,

$$\Delta f_d^2 = \frac{\beta AE (2k-1)^2 \pi^2}{4\ell(0.5M)} \left[\frac{b_o}{\ell} + \frac{1}{(2k-1)\pi} \left\{ \sin \frac{(2k-1)\pi b_o}{\ell} \cdot \cos \frac{(2k-1)\pi \ell_o}{\ell} \right\} \right] \quad (21)$$

As before, for a widespread uniform reduction in AE, substituting, $l_0 = b_0 = \ell/2$,

$$\Delta f_d^2 = \frac{\beta AE (2k-1)^2 \pi^2}{4\ell M} \quad (22)$$

The ratio of Eigen value reduction is,

$$\frac{\Delta f_d^2}{f_{ud}^2} = 2\beta \left[\frac{b_o}{\ell} + \frac{1}{(2k-1)\pi} \left\{ \sin \frac{(2k-1)\pi b_o}{\ell} \cdot \cos \frac{(2k-1)\pi \ell_o}{\ell} \right\} \right] \quad (23)$$

A five-segment rod is taken for validation in the forward problem. The damage positions and extent are kept as un-symmetric. A 5.0 m bearing

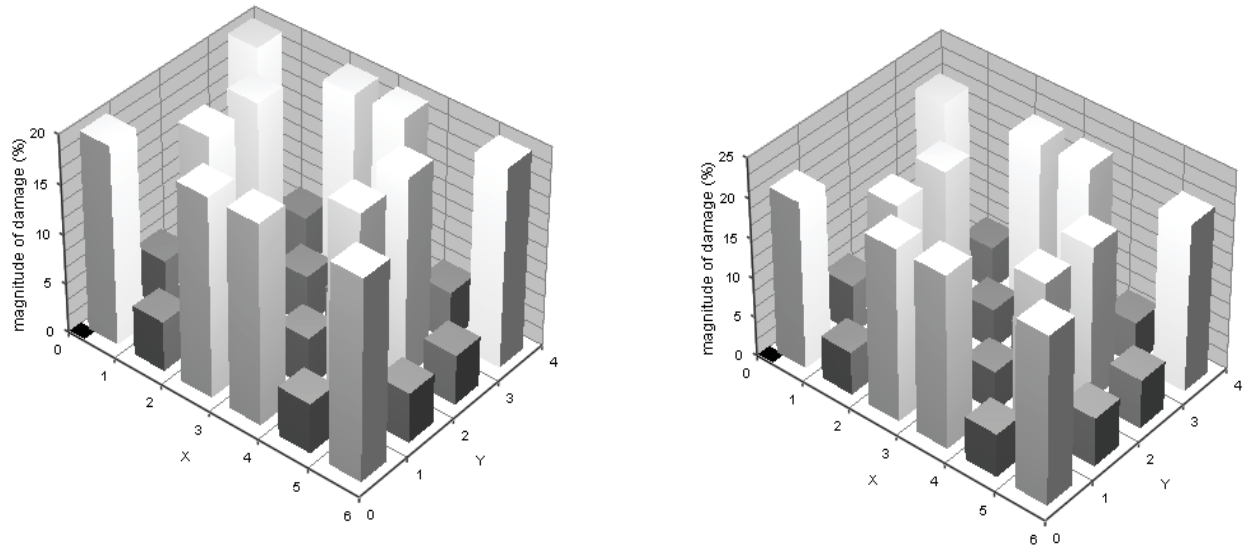


Figure 7.1: Comparison of Damage Predicted by Perturbation Analysis with Actual Damage Values for Case-1

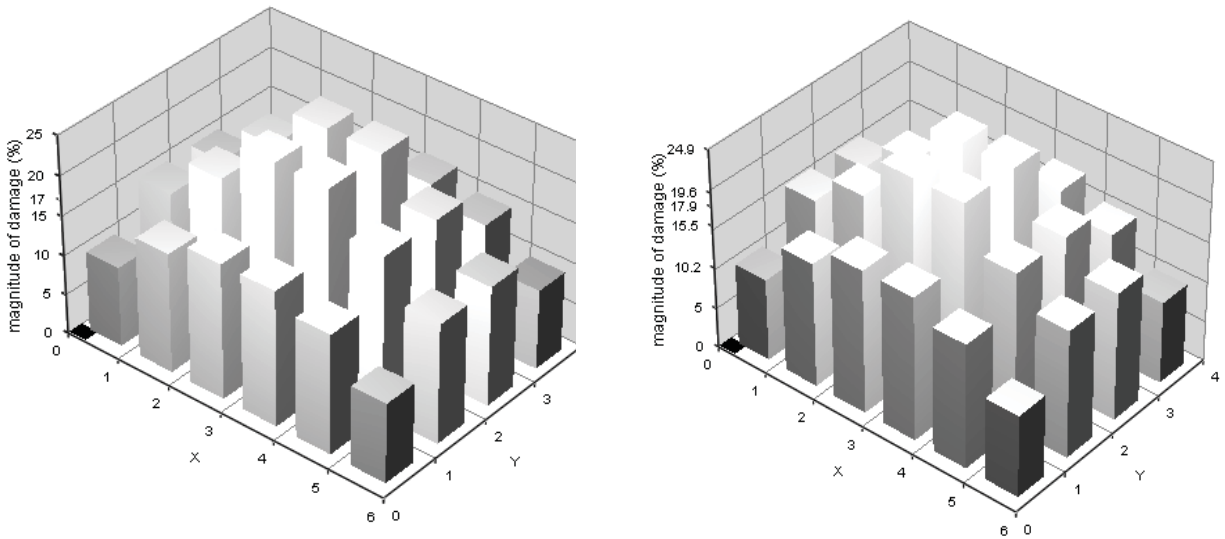


Figure 7.2: Comparison of Damage Predicted by Perturbation Analysis with Actual Damage Values for Case-2

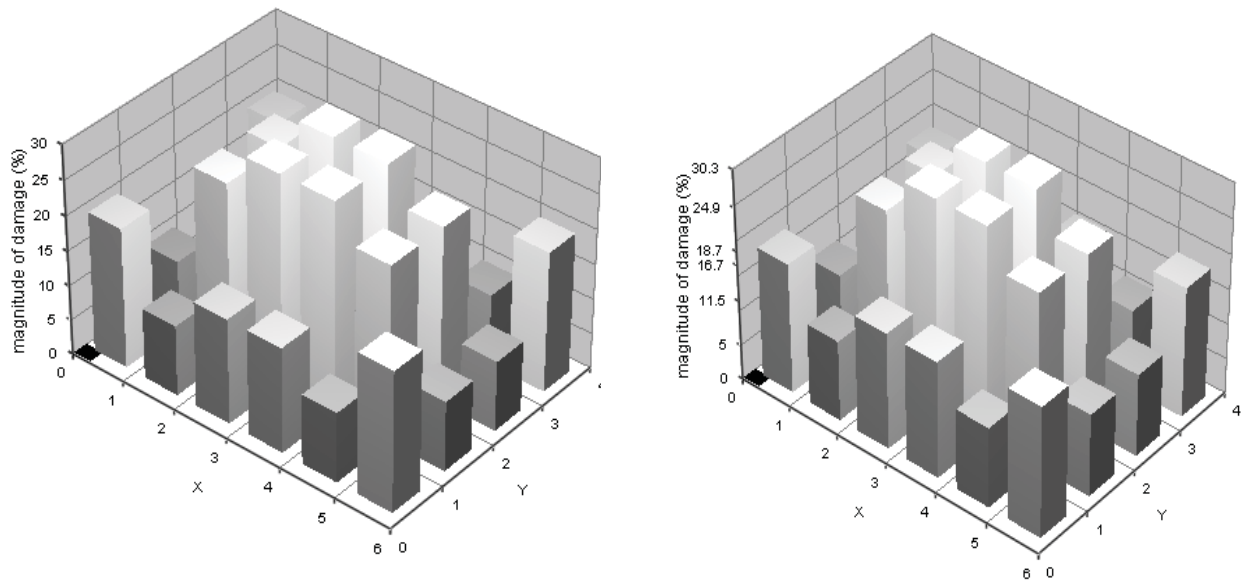


Figure 7.3: Comparison of Damage Predicted by Perturbation Analysis with Actual Damage Values for Case-3

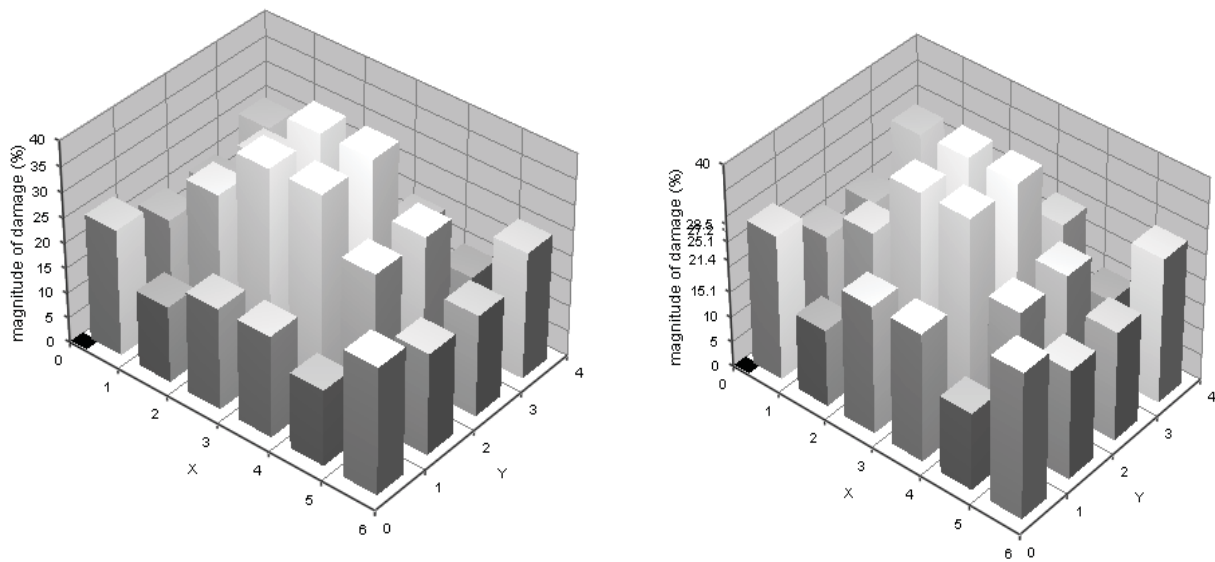


Figure 7.4: Comparison of Damage Predicted by Perturbation Analysis with Actual Damage Values for Case-4

pile with a 300 mm diameter is taken as a case study.

Three length types chosen are, $L1 = \{0.5, 0.75, 1.0, 1.25, 1.5\text{m}\}$, $L2 = \{0.8, 0.9, 1.0, 1.1, 1.2\text{m}\}$ and $L3 = \{0.75, 1.0, 0.75, 1.0, 1.5\text{m}\}$. For each of these length types four damage profiles are used for verification. This include, $D1 = \{0.10, 0.20, 0.0, 0.15, 0.05\}$, $D2 = \{0.15, 0.25, 0.05, 0.20, 0.10\}$, $D3 = \{0.30, 0.35, 0.15, 0.20, 0.10\}$, $D4 = \{0.35, 0.40, 0.15, 0.25, 0.20\}$.

Tables 3 – 5 give the comparison of damaged frequencies from perturbation equation and finite element analysis for length types L1, L2 and L3 respectively.

Figures 8-9 show the variation in frequency reduction (for five modes) for three magnitudes of damages, namely, 0.10 and 0.30 respectively. The position and extent of damage is the dependent variable in each graph.

7.2 Axial Rod Element – Inverse Problem

The methodology of the inverse problem for an axial rod is essentially same as beam or plate. The difference is that symmetry of damage cannot be assumed. In the case of the sensitivity matrix for the beam and plate, for equal-length of damage segments, the matrix columns are mirror images. The physical reason being that, identical damages on equi-length segments, symmetric with reference to centre, produce same drop in frequencies. Hence, if we do not make use of symmetry explicitly, the matrix is singular and cannot be solved. Hence the sensitivity matrix is generated for only one half of the beam (or one-quarter of plate) and multiplied by two (or four in the case of plates) and made use of. In cases, where, there is no-symmetry in damages, segments have to be unequal lengths and un-symmetric with reference to the centre. Though not so explicit, the columns of sensitivity matrix of the axial rod element, generated from quarter (odd-multiples of) sine curves are linearly dependent (half of them at least) and un-symmetry of positions and extents have to be adopted. It is better to fall back upon the engineering judgement that more the damage, less will be its length. Hence four different length types are used in the inverse analysis for the axial rod.

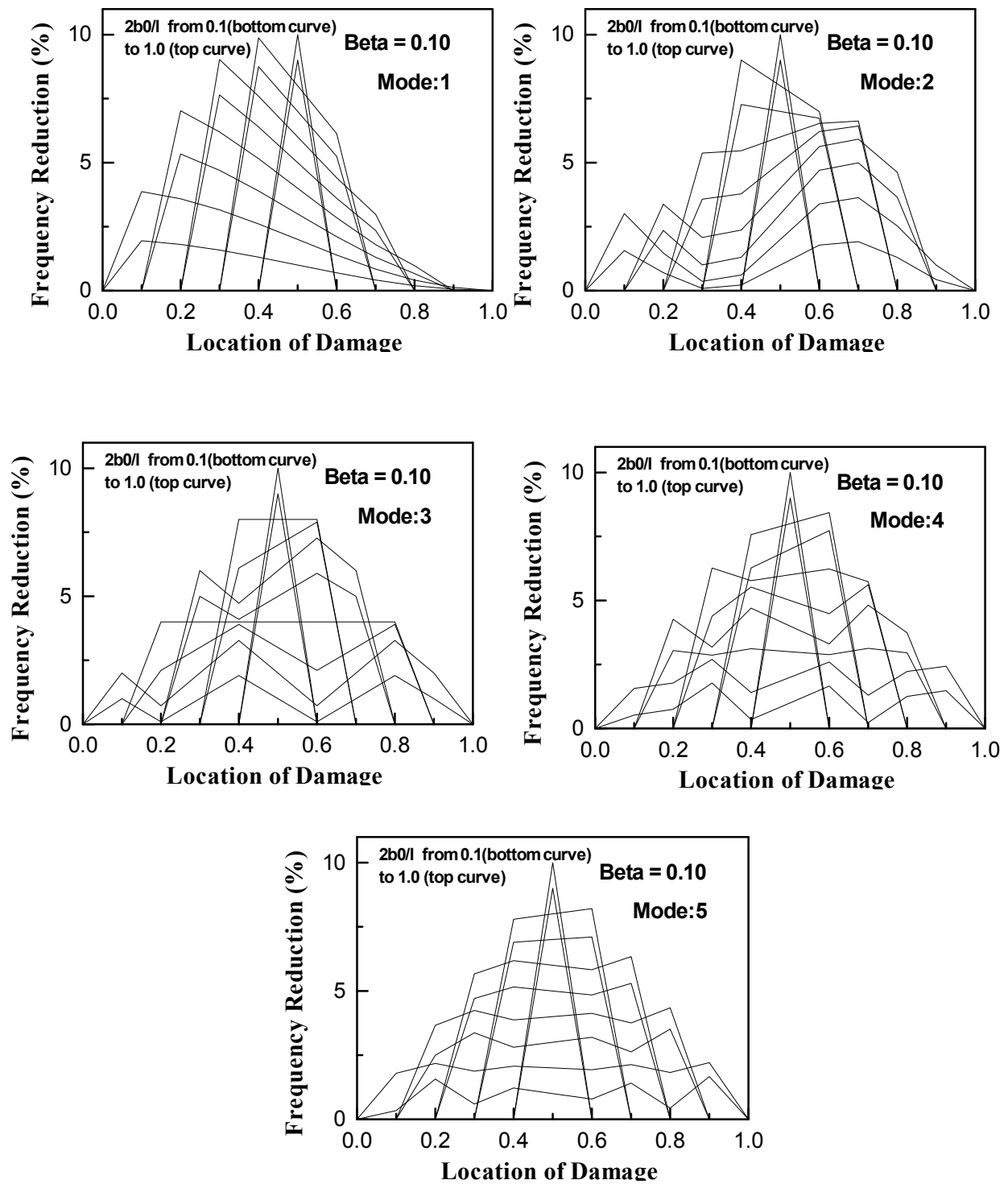
Fig. 10 shows the length types used. The damage patterns are similar as used in forward analysis. Retrieved damages, as compared to the actual damages are shown in Figs 11 to 13, for the three length types.

8 Effect of Measurement Errors in Damage Prediction

Any damage prediction work is in-complete unless the effect of errors on the measured signals is investigated. There could be two sources of errors in a bridge response and frequency computation using FFT (Fast Fourier Transform). Typical medium span bridges have low frequencies ranging from 3 to 5 Hz in the first flexural mode and 75-125 Hz in the fifth mode. Typically 16384 (2^{14} in octave range) points could be easily acquired either in ambient or in forced excitation modes. This is equivalent to 6400 lines in frequency scale. To capture up to 125 Hz, the frequency span could be set as 200 Hz with an effective sampling rate of $2.56 \times 200 = 512\text{Hz}$. Thus the resulting frequency resolution is 0.08 Hz. Hence the maximum error possible is 0.04 Hz. For a 5 Hz system, this is equivalent to an error of 1%. A still lower resolution is also achievable if FFT block could be raised beyond 2^{14} data points. However, in the higher modes this error ratio may fall by more than an order of magnitude. The second error source is through reduced energy levels at higher modes than compared to lower modes. Thus the two error sources affect each mode differently and in the present study a uniform error of 1% for all modes are assumed.

The error vectors injected into the simulation is (a) E1: uniform 1% rise in Eigen values (b) E2 : uniform 1% drop (c) E3: An oscillating 1% (+1%, -1%, +1%, -1%, +1%) and (d) E4 : another oscillating 1% drop (-1%, +1%, -1%, +1%, -1%).

Many damage patterns are subjected to these error profiles and typically those, which show large deviations are shown. Fig-14 shows the performance of a simply supported beam under the influence of errors. Fig-15 and Fig-16 show the performance of the axial rod element under the influence of errors. Similar curves for plates are in Figs 17 and 18.

Figure 8: Frequency Reduction of a Rod Element with Variation in position and Extent of Damage ($\beta=0.10$)

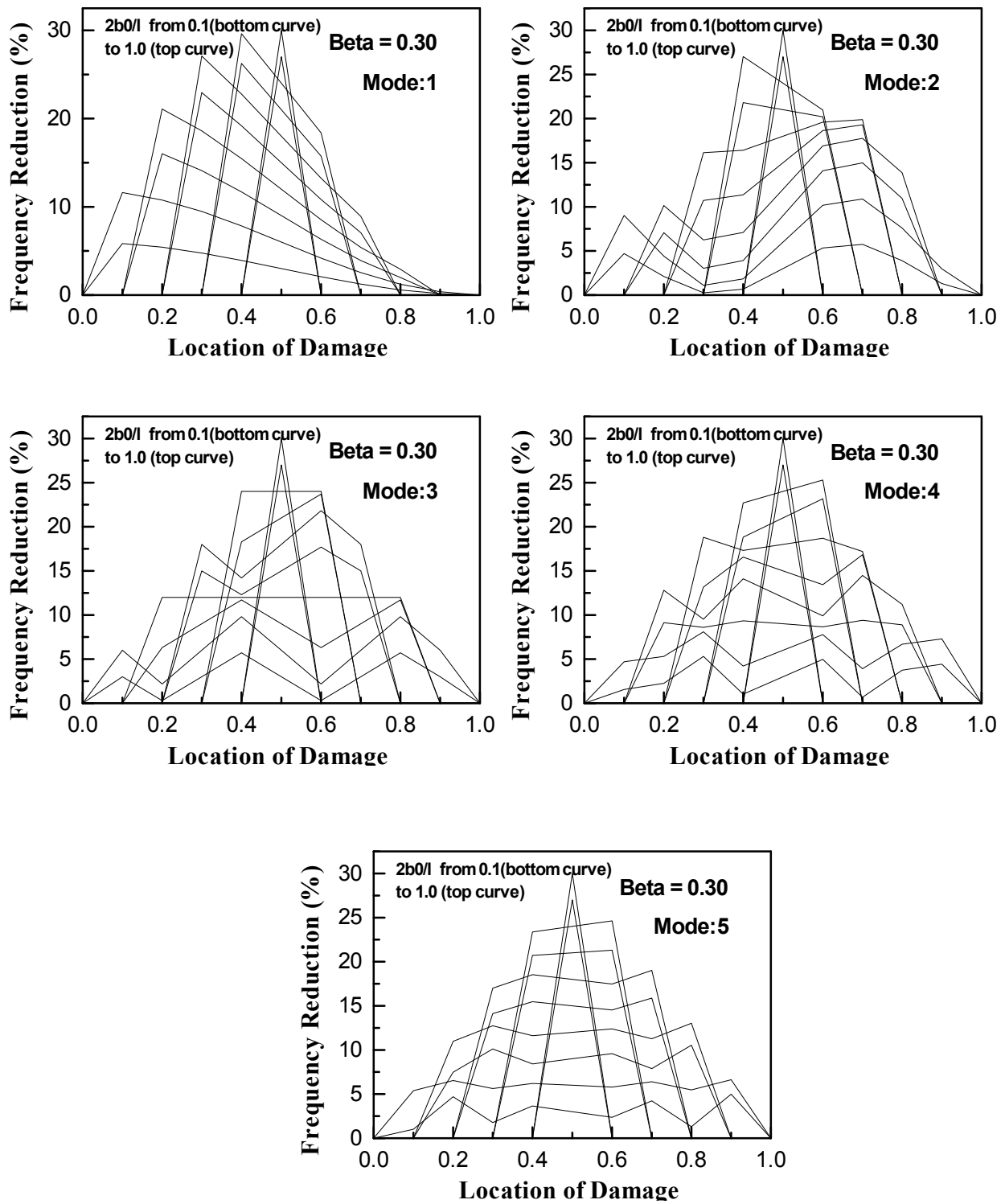


Figure 9: Frequency Reduction of a Rod Element with Variation in position and Extent of Damage ($\beta=0.30$)

Table 3: Comparison of Frequencies for Rod Element after Damage (Length Type – I)

Mode No.	Natural frequency(f_d) For case-1		Natural frequency(f_d) For case-2		Natural frequency(f_d) For case-3		Natural frequency(f_d) For case-4	
	Perturb.	FEM	Perturb.	FEM	Perturb.	FEM	Perturb.	FEM
1	163.74	163.11	159.10	158.40	150.73	149.66	146.94	145.41
2	488.44	487.43	474.42	473.32	461.48	459.72	443.02	442.01
3	837.84	836.49	815.16	813.69	788.18	786.24	762.21	760.52
4	1158.56	1156.11	1126.40	1123.73	1093.43	1086.46	1056.70	1048.02
5	1480.13	1475.32	1438.50	1433.32	1394.67	1385.47	1346.32	1337.15

Table 4: Comparison of Frequencies for Rod Element after Damage (Length Type – 2)

Mode No.	Natural frequency(f_d) For case-1		Natural frequency(f_d) For case-2		Natural frequency(f_d) For case-3		Natural frequency(f_d) For case-4	
	Perturb.	FEM	Perturb.	FEM	Perturb.	FEM	Perturb.	FEM
1	163.23	162.64	158.57	157.93	148.57	147.65	144.67	143.24
2	490.74	489.80	476.79	475.76	457.91	457.56	444.57	444.19
3	834.49	831.90	811.72	808.89	772.47	767.15	755.36	747.58
4	1145.33	1142.77	1112.78	1110.03	1064.03	1059.25	1033.50	1027.75
5	1480.00	1478.35	1438.37	1436.60	1375.40	1372.87	1340.58	1336.87

Table 5: Comparison of Frequencies for Rod Element after Damage (Length Type – 3)

Mode No.	Natural frequency(f_d) For case-1		Natural frequency(f_d) For case-2		Natural frequency(f_d) For case-3		Natural frequency(f_d) For case-4	
	Perturb.	FEM	Perturb.	FEM	Perturb.	FEM	Perturb.	FEM
1	162.45	161.90	158.19	157.61	148.09	147.18	143.90	142.57
2	491.47	490.59	472.53	471.31	458.65	458.11	444.61	444.09
3	834.90	832.23	808.20	806.02	772.23	766.66	754.02	746.10
4	1138.71	1136.93	1113.19	1112.06	1060.58	1056.55	1027.47	1022.84
5	1480.91	1478.34	1447.46	1444.60	1376.27	1372.43	1340.56	1335.58

- (a) Error injection affects the larger damage regions less.
- (b) Low damage regions show large prediction errors. For example, a 5% damage zone is depicted anywhere between 3-7%.
- (c) If an averaging is done on the generated damage data, there is a tendency to the error minimization, similar to a Gaussian error getting cancelled after many averages.
- (d) For the three structural elements, susceptibility to measurement error is more for plates, less for beam and the least for rods.

9 Damage Estimation of a Discrete Structure

The structures taken up hitherto for damage estimation from Eigen value sensitivity method are continuum structures for which closed form expressions for Eigen function is readily available. Towards illustrating the versatility of the method for all kinds of structures, where Eigen function is readily not available, a discrete torsionally-sensitive L-type frame is taken (Fig. 19). The frame is un-symmetric in plan and consists of 3 bays along X-direction and 4 bays along Y-direction. Width of each bay is 4.0 m, thus the plan dimensions are 16 m \times 12 m. There are three floor each having a storey-height of 3.0m. The structure is a reinforced concrete type with column dimensions of 400 mm \times 400 mm for all columns and 300 mm X 300 mm for all beams.

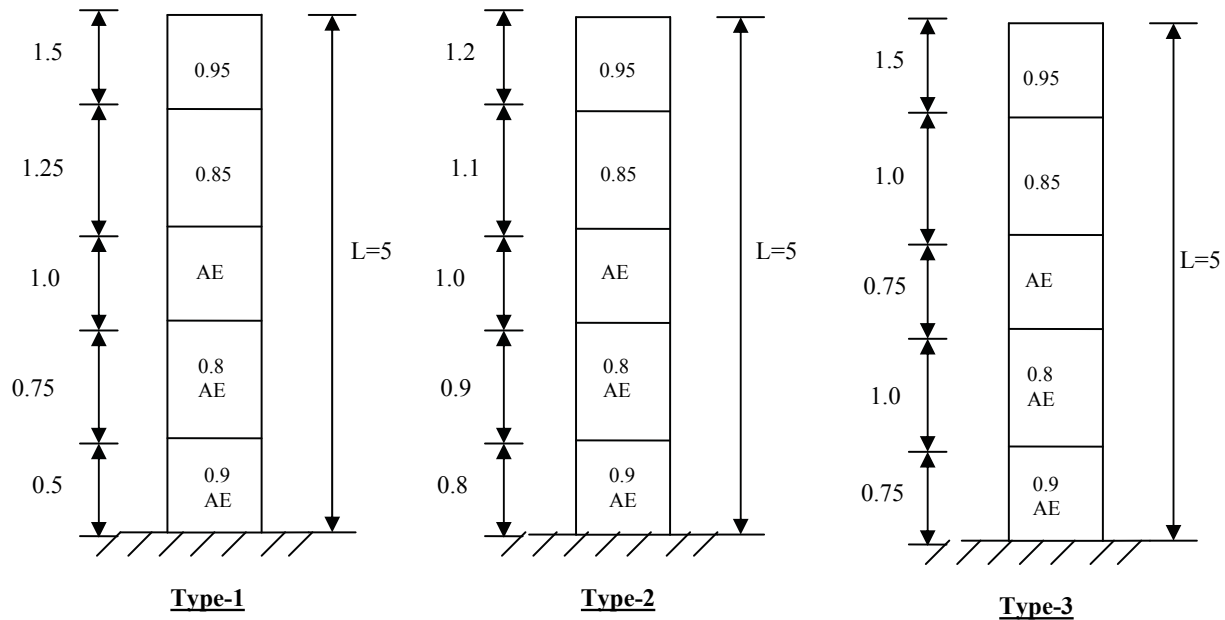


Figure 10: An Example for Validation of the Developed Method for an Axial rod

It is assumed that the structure is subjected to a seismic excitation and the bottom most two floors are assumed to be damaged under the action of a seismic force. The third floor is assumed as undamaged. The purpose of the exercise is to estimate the floor-wise damage suffered by the structure. This means that a quantity of a percentage damage for each floor shall be specified but its actual distribution for individual columns or beams shall be a function of the ratio of the force (or displacement) demand of the individual element to its force (or displacement) capacity. The Eigen value solution of the virgin frame, in its healthy state is initially carried out and its frequencies and mode shapes are obtained. Then a uniform flexural rigidity gain of 5% for all beams and columns at a specified level is imposed and the frequencies and mode shapes are again computed. Using the changes in the Eigen values as the ratio of initial Eigen values, a column of the sensitivity matrix is constructed. Then changing the flexural rigidity gain to the next floor, yet another column is created. The number of rows in the columns are the number of frequencies for which the change in Eigen values can be measured.

For the illustrative example, Table-6 give the fundamental frequencies :

Numerically computed sensitivity matrix, A is as follows :

$$[A] = \begin{bmatrix} 0.4754 & 0.3039 \\ 0.4853 & 0.3113 \\ 0.4930 & 0.3188 \\ 0.3565 & 0.1388 \\ 0.3569 & 0.1400 \\ 0.3558 & 0.1484 \end{bmatrix} \tag{24}$$

In the [A] matrix, the first column corresponds to first floor and the second column corresponds to second floor. In the simulation study, a damage of 28% is inflicted for the first floor and 14% for the second floor. The example is essentially over-determined with more information available and less un-known values sought. The frequencies are computed and given as input and the least square solution of the problem as given in the following equation has yielded damage values of 30% and 14% respectively for first and second floors, thus illustrating the efficacy of the method developed.

$$[A] \{\beta\} = \{\epsilon\} \tag{25}$$

$$\{\beta\} = ([A]^t [A])^{-1} [A]^t \{\epsilon\}$$

Let us discuss the practical viability of the method in which the Eigen sensitivity is generated by an

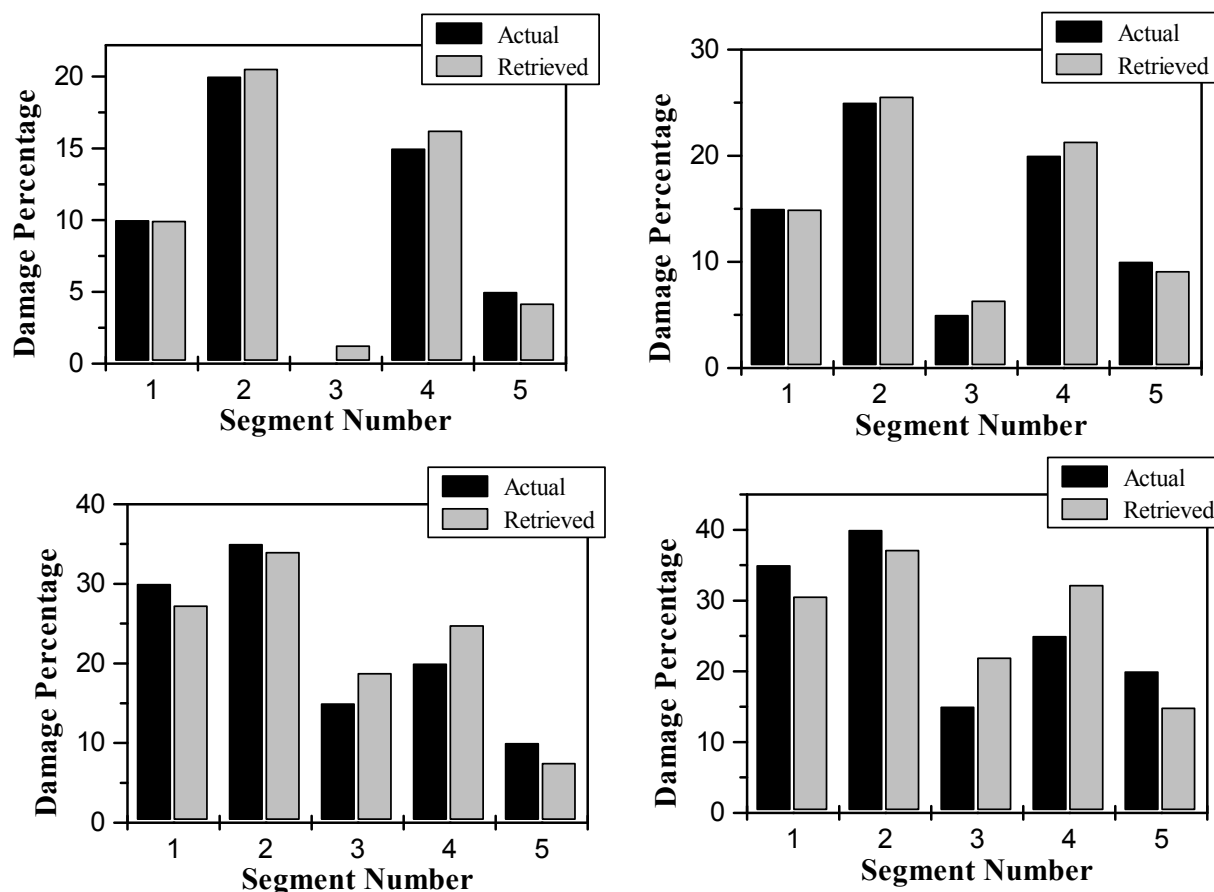


Figure 11: Comparison of Damage Predicted by Perturbation Analysis for an Axial Rod with Actual Damage Values for Length Type-1

Table 6: Frequencies of the example discrete building structure

Mode Number	Mode Description	Frequency (Hz)
1	Pre-dominant X-Axis –First bending mode	1.568
2	Pre-dominant Y-Axis–First bending mode	1.596
3	Torsional first mode	1.771
4	Pre-dominant X-Axis –Second bending mode	4.928
5	Pre-dominant Y-Axis–Second bending mode	4.984
6	Torsional second mode	5.536

apparent increase of stiffness (and not reduction), initially and this is later on used to predict the loss in the stiffness, with sufficient accuracy. It is possible to extend this method as a field method. However, un-like computations, a stiffness gain are invariably accompanied by mass increase and suitable corrections are required. This important issue will be covered in a subsequent paper.

10 Damage Estimation through a neural network scheme

Sensitivity equation, connecting the magnitudes of damage with the frequency reduction is computed assuming a linear relationship between both, experimentally or analytically. However, the limitation, as indicated by this study, is that the magnitude of damage shall be less than 30%, so that the assumption of linearity is valid. The

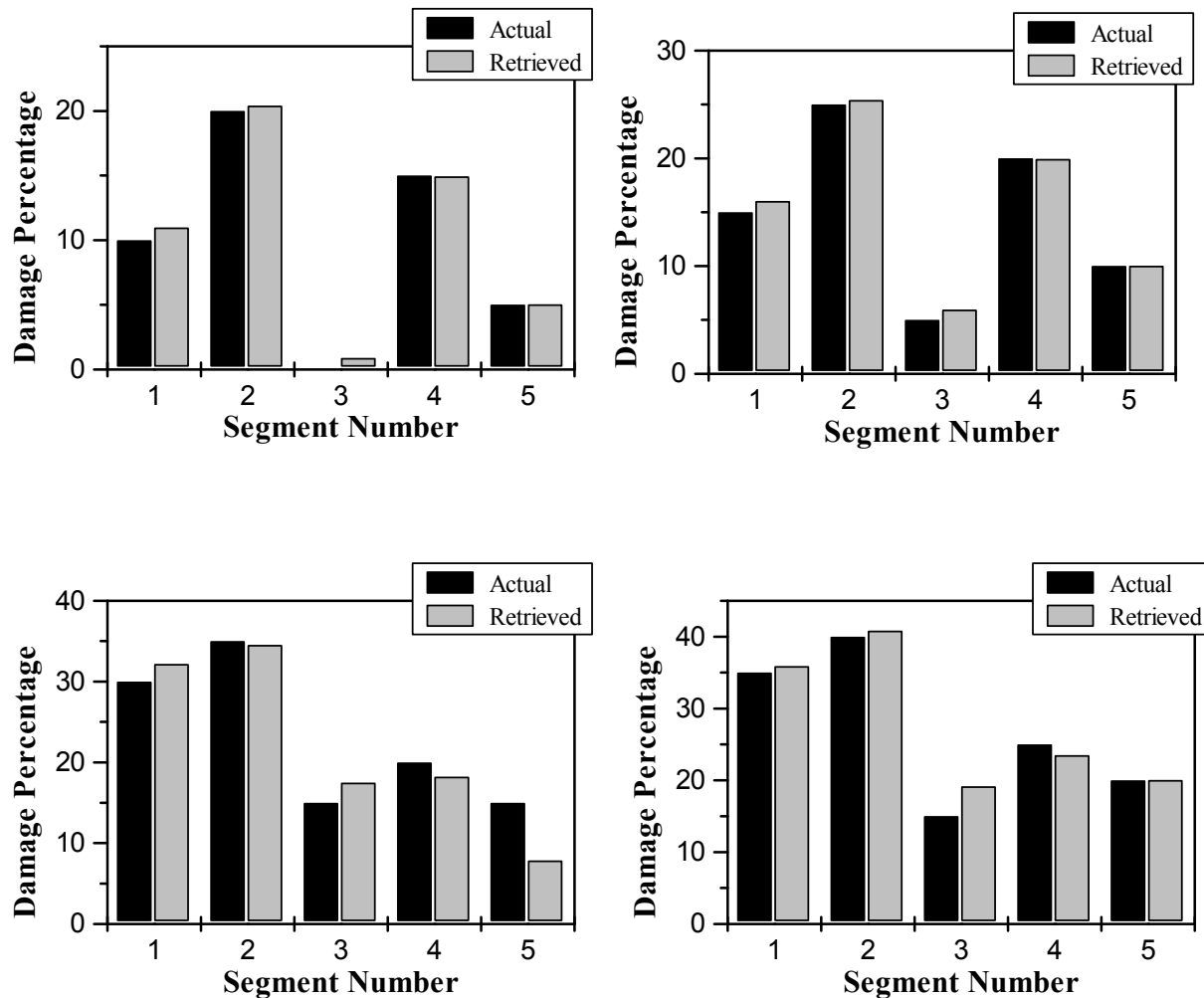


Figure 12: Comparison of Damage Predicted by Perturbation Analysis for an Axial Rod with Actual Damage Values for Length Type-2

generalised solution strategy hence may be based on a neural network scheme, which may take care of both linearity as well as non-linearity. An artificial neural network based radial basis function network (RBFN) is trained with a database of known frequency-damage pair of vectors such that for any known vector of frequency change ratios, damage vector can be evaluated. Typical error analysis due to measurement noise is also carried out.

In this study, the bridge is considered as a simply supported beam and the dynamic analysis (for extracting the natural frequencies) is carried out using an in-house program and based on finite element method. The input parameters are (a) mag-

nitude of damage, (b) location of damage, and (c) extent of damage. The output obtained is a set of natural frequencies for the flexural mode of the beam. The architecture of an RBFN network consists of an input layer, a hidden layer with a radial activation function and an output layer. The network structure uses non-linear transfer function which may be a typical Gaussian function after the input layer and one more linear transfer function between the hidden and output layers (Purelin() as in Matlab [24]). Reason being that, input spaces non-linearly mapped onto high dimensional domain are likely to be linearly separable. This non-linear transfer functions are symmetric, maximum at peak points and positive val-

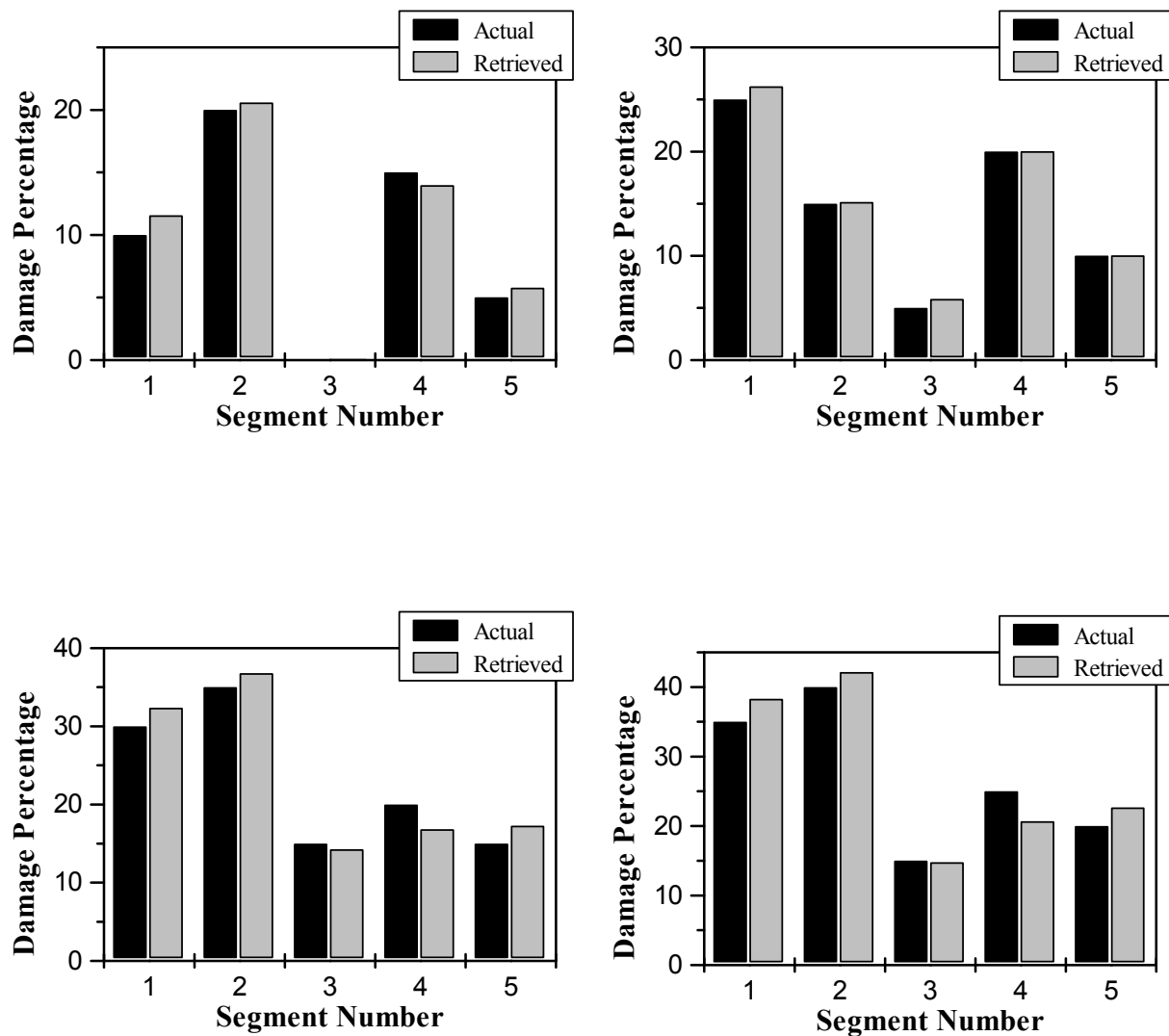


Figure 13: Comparison of Damage Predicted by Perturbation Analysis for an Axial Rod with Actual Damage Values for Length Type-3

ued. The two main parameters that characterize these functions are their centres and spread values. The spread values for minimum error are estimated by a trial and error process.

Problem considered is similar to the one previously discussed and solved using the Eigen sensitivity matrix. The same ten segment beam is considered with symmetry in damage but the solution is through a trained neural network. Hence the number of un-known values are five (β_i , where 'i' ranges from 1 to 5) and hence information on the five frequency ratios are to be made available. EI

reduction is assumed in three steps, 0% or 15% or 30% for each beam segment. This means, for a 10 segment beam, symmetrically damaged, there are 3^5 (243) training sets.

For checking the performance of neural networks, induced damage vectors are given as, $D1 = \{5, 35, 0, 15, 5\}$, $D2 = \{35, 5, 35, 15, 0\}$, $D3 = \{5, 18, 30, 18, 5\}$ and $D4 = \{30, 20, 12, 5, 0\}$. Fig. 20 shows the comparison of induced and retrieved damage values. The frequency measurement error analysis has also been done for four types of error patterns, E1: uniform +1% , E2: uniform -1%, E3:

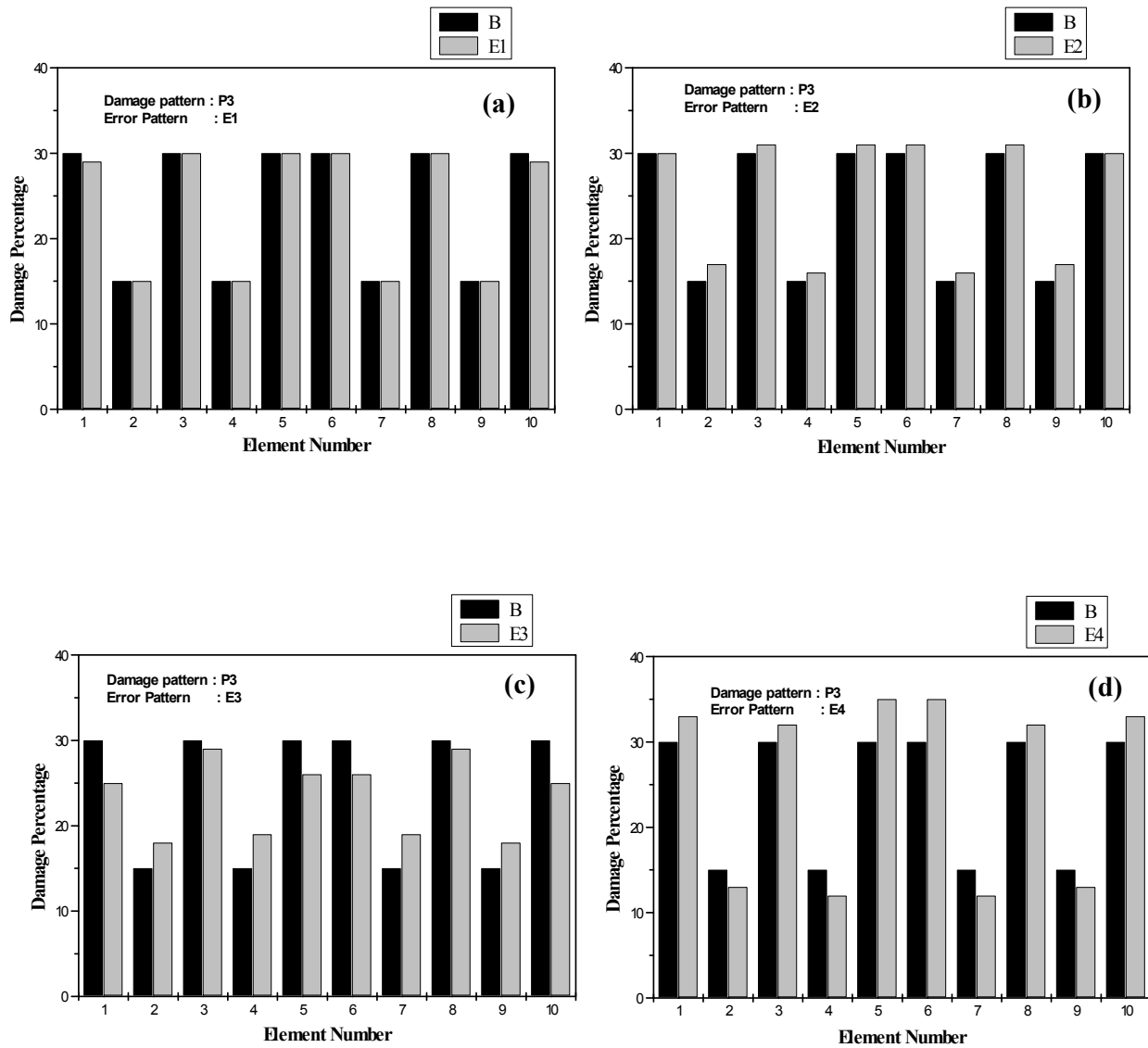


Figure 14: Performance of First-Order Perturbation based damage identification Method with Measurement errors (Beam)

fluctuating +1%, -1%... and E4 fluctuating -1%, +1% and so on. Fig. 21 shows the comparison of retrieved and induced damage patterns under the presence of measurement errors.

10.1 Discussion of Results

Three classes of structural elements and a building structure are taken up for the study which involve computation of frequencies for a known amount and position of damage (forward problem) and re-generation of flexural or axial rigidi-

ties, once the changes in frequencies are known (Inverse problem). These include a simply supported beam, thin plate element and an axially loaded element. The known expressions for the mode shapes and strain energy for the two cases are made use of to derive the suitable expressions. Series of damage patterns are tested for the validity of those developed expressions, which relate the position and magnitude of the damage to the changes in Eigen values.

The following points are directly due to the results

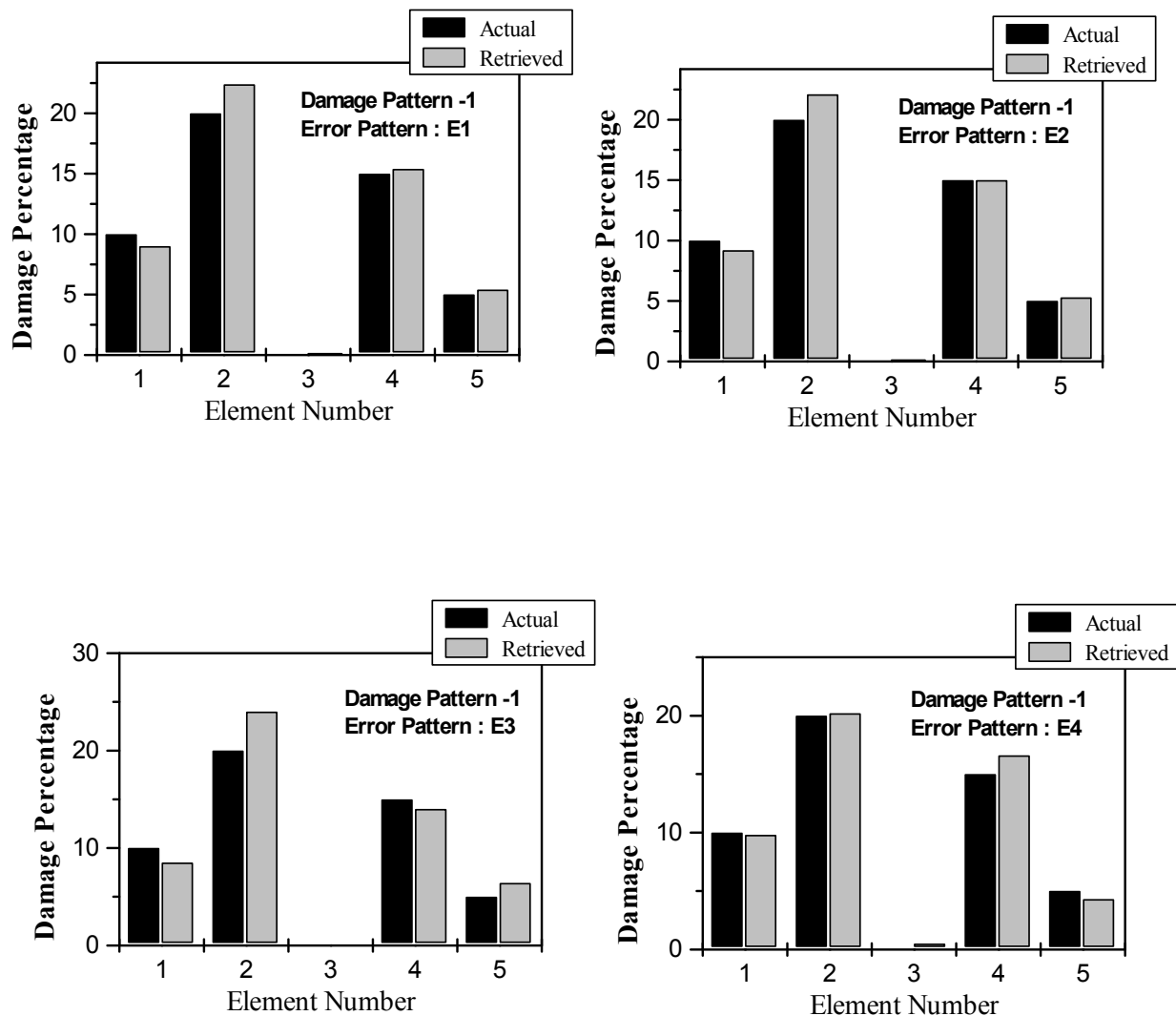


Figure 15: Variation of Retrieved Damages for an Axial Rod in the Presence of Measurement Error - Damage Pattern-1

based on Fig. 4, Fig. 8 and Fig. 9.

- (1). Frequency reduction monotonically increases with increased percentage of local damage (β).
- (2). When the extent of damage is small, compared to the pseudo-span of the structure, (Pseudo span is the length between adjacent curvature nodes, $\frac{\ell}{n}$, n =No of half cycles) frequency reduction is more, when the location of damage coincides with the anti-node (or peak curvature point) of the beam. Conversely, when the extent of damage is more compared to the pseudo-span of the struc-

ture, ($\frac{\ell}{n}$), frequency reduction is more, when the location of damage coincides with the node (or zero curvature point) of the beam. When the extent of damage is equal to the pseudo-span, the variation is invariant with reference to the position of damage.

- (3). For small extent of damage, frequency reduction varies rapidly depending on the location of the damage. However for large extent of damage, frequency reduction varies less rapidly, with the location of damage.
- (4). Frequency reduction is more in the first mode, as compared to other modes, for the

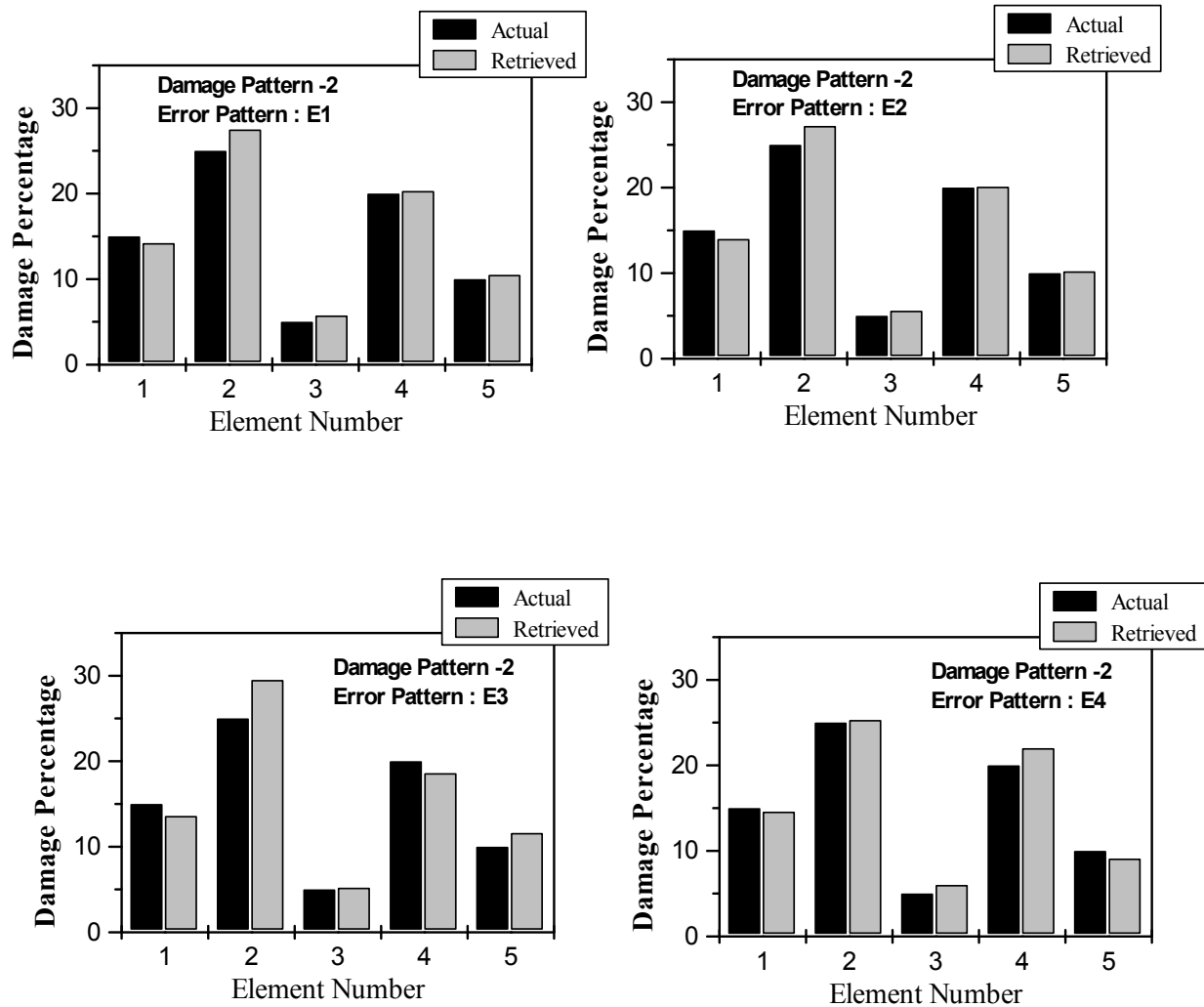


Figure 16: Variation of Retrieved Damages for an Axial Rod in the Presence of Measurement Error - Damage Pattern-2

same magnitude of damage, extent of damage and critical position of damage.

The derived forward equation, produces, generally, an error of less than 0.3% in the estimation of frequencies for $\beta < 20\%$, an error less than 0.5% for $20\% < \beta < 30\%$, less than 1.0% for $30\% < \beta < 40\%$ and more than 1.0% for $\beta > 40\%$. The equation always gives rise to upper-bound values of frequencies or in other words actual changes in frequencies get reduced. The error may look apparently low, but what matters, is the comparison of actual changes in frequencies, *vis-à-vis* those predicted by the perturbation equation. For the inverse problem, in the absence of measurement errors, re-generation of flexural or axial rigidities

up to $\beta > 40\%$ produces tolerable errors. Beyond 40% of damage, regions of low strain energy density (supports for beams and plates and free-ends for axial rods) show larger deviations and the damages are over-estimated. The effect of artificial error-ingress affects regions of low or zero damage. Out of the three classes of structures, plate suffers more fluctuations, particularly at edge elements. The best way is to do averaging at inverse stage as well as removing those elements which are not likely to suffer damage, from the equations, using some form of engineering judgement.

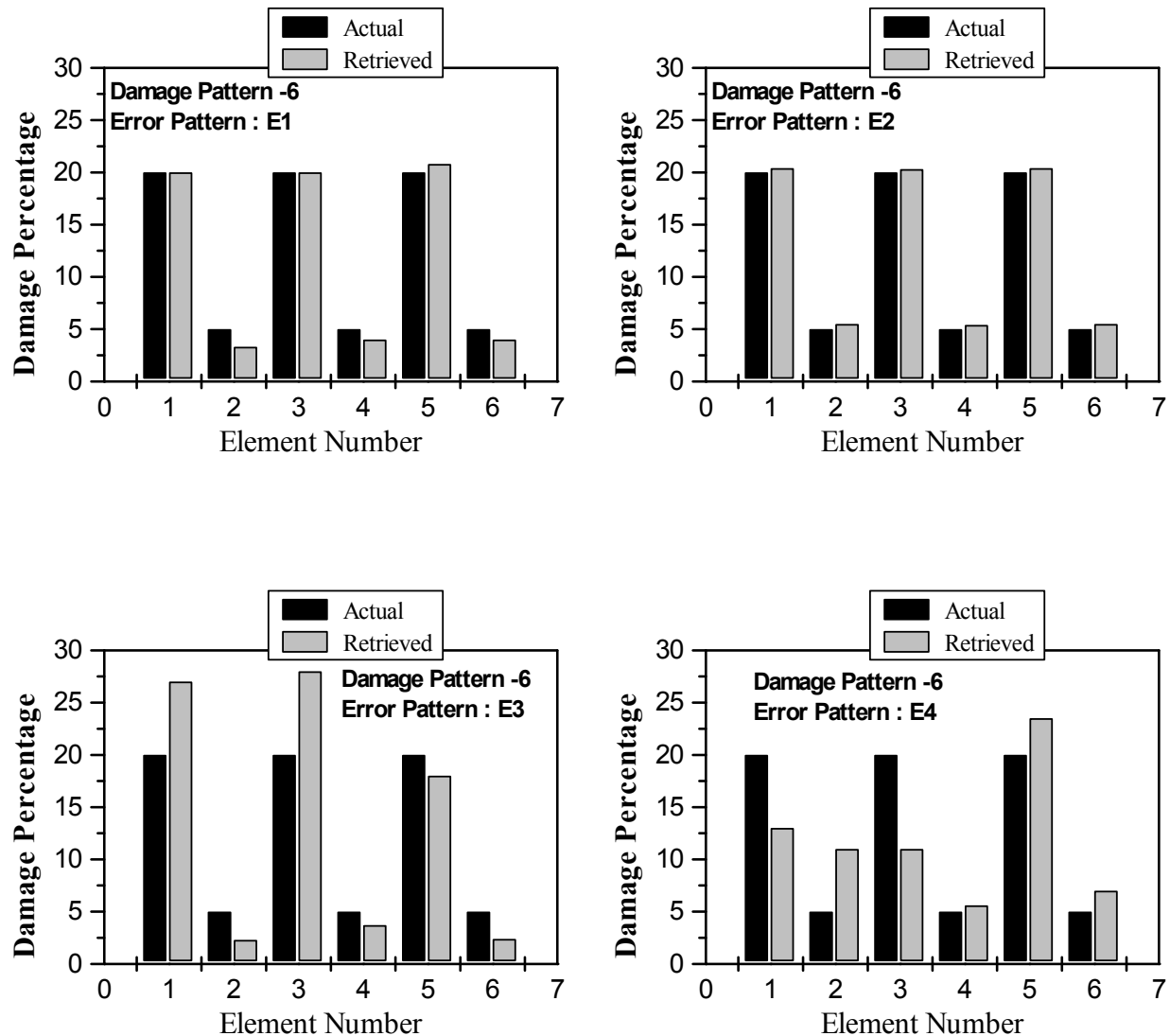


Figure 17: Variation of Retrieved Damages for a Plate in the Presence of Measurement Error - Damage Pattern-1

10.2 Extension of damage identification methodology for general classes of structures

The methodology of damage detection for a generalised class of structure will be on lines similar to the one adopted for the discrete framed structure and is stated as follows:

- The regions of likely damage are marked. Suppose there are ' n ' regions of suspect at least ' n ' frequency change information has to be available. If more information is available on frequency changes, then a least-square

based solution is to be resorted.

- Sensitivity of the frequency change to a unit change in flexural rigidity (or axial rigidity or a general stiffness) is to be generated either numerically or using closed-form expressions.
- The sensitivity matrix is either inverted (for an evenly determined system) or a least square based over-determined solution methodology is adopted to get the damage values.
- If the solution predicts un-reasonable values

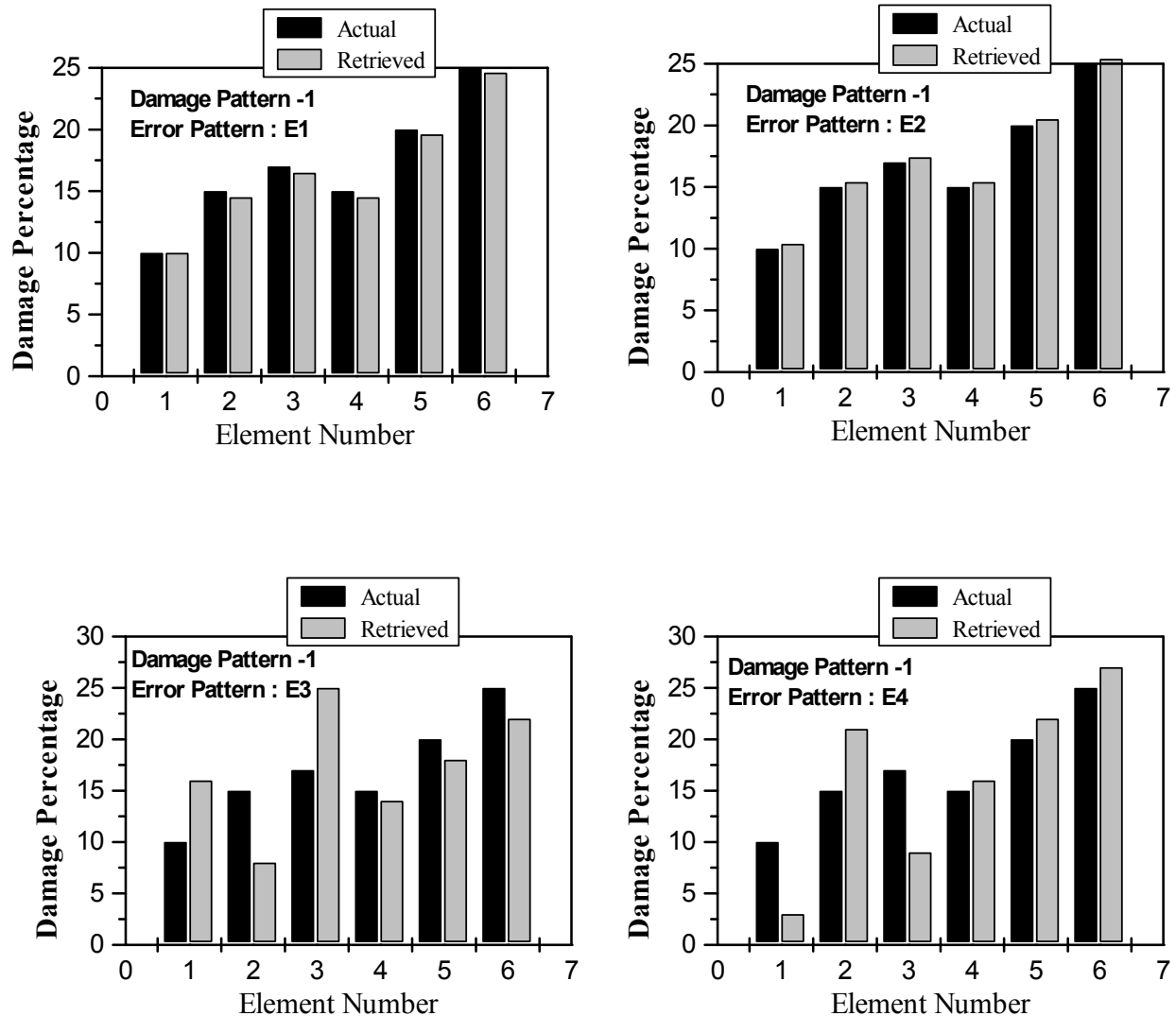


Figure 18: Variation of Retrieved Damages for a Plate in the Presence of Measurement Error - Damage Pattern-2

like growth in a section or negative damage, then these regions are imposed to be of zero damage and the solution is repeated.

10.3 Damage identification in regions of less strain energy density

Regions of least strain energy density are likely to show more fluctuations in the predicted damage, than those regions of high strain energy density. Typically these are the mid-span regions of simply supported beams or plates and support regions of cantilever. Normally the structural design methodology is such that these regions of high

strain energy density are also the most likely regions of damage. Hence the most damaged regions will be automatically predicted with high reliability. However in cases of high damage in support regions of a simply supported beams or the tips of cantilever, if the damage magnitude is large (more than 10%), then the prediction is generally fine. However if the damage magnitude is small and if it occurs in these less dense areas, alternative damage detection using local parameters like strain, slope change and modal curvatures have to be adopted as damage indicating parameters rather than natural frequencies.

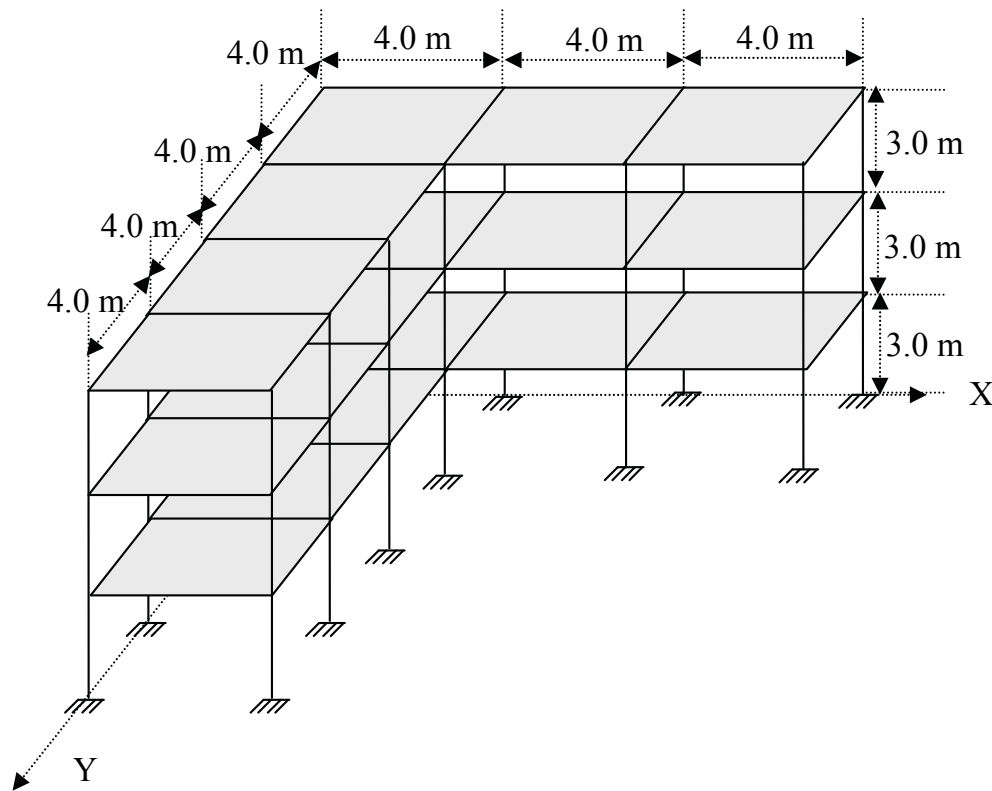


Figure 19: Illustrative Structure for Damage Estimation - Discrete Structure

11 Conclusions

Closed-form expressions based on first-order perturbation technique, relating the reduction in natural frequencies to the local reduction in stiffness are derived for a simply-supported beam, plate and an axial rod element. The inverse problem of determining the damage from the known changes in frequencies is out-lined for a smeared damage model. This could be used in typical infrastructural management programs such that the natural frequencies obtained remotely from a site could be integrated and damages could be simultaneously got, as a first-level screening tool. In addition to classical cases, the methodology is proven for a discrete structure to estimate the floor-wise damage of an un-symmetrical building. Sensitivity matrix derived computationally in this case using an increased stiffness values, is adoptable in practical cases using experimental evaluation with mass correction. Near-support zones for the beam and plates and near-free-end in the case of

rod, where the strain energy density is low, effect of measurement noise may be more. It is recommended that an engineering judgement on the possible damage zones could be made initially, so as to avoid errors. Lastly, a neural network based damage identification methodology is also discussed, wherein the assumption of linearity between damage and Eigen values is defied.

References

- Araujo Dos Santos, J.V., Mota Soares, C.M., Mota Soares, C.A., Pina, H.L.G.** (2000): Development of a Numerical model for the damage identification on composite plate structures, *Composite Structures*, 48, 59-65.
- Castro, E., Garcia Hernandez, M.T., Gallego, A.** (2007): Defect identification in rods subject to forced vibrations using the spatial wavelet transforms, *Applied Acoustics*, 68, 699-715.
- Choi, S., Park, S., Yoon, S., Stubbs, N.** (2005): Non-destructive damage identification in plate

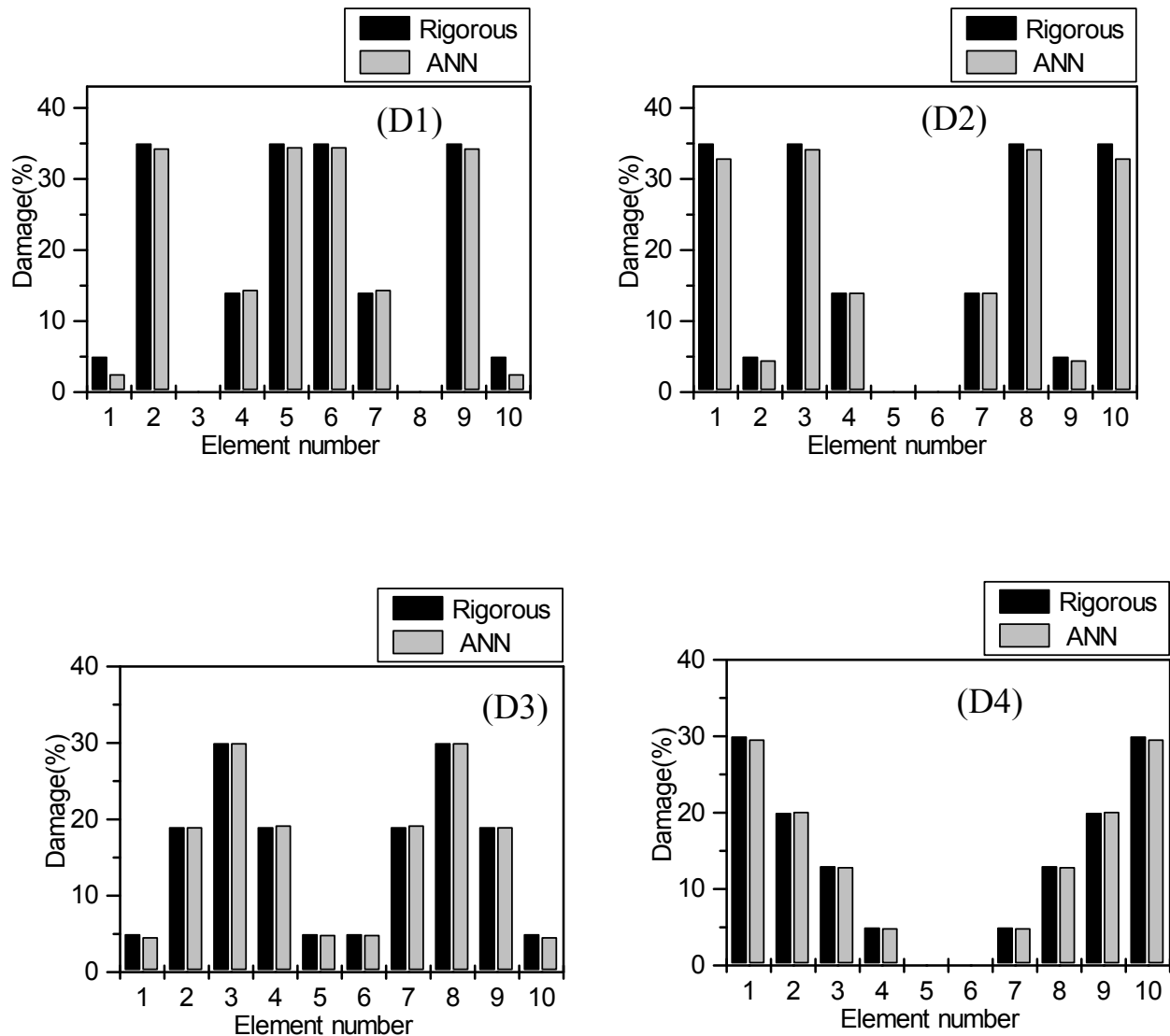


Figure 20: Comparison of Damage Predicted by artificial neural network with the induced damage Values

structures using changes in modal compliance. *NDT&E Intl.*, 38, 529-540.

Doebling S.W., Farrar C.R., Prime M.B., Shevitz, P.W. (1996): Damage Identification. Health monitoring of structural and mechanical systems from changes in their vibration characteristics – A literature review, Los Alamos National Laboratory, Los Alamos, New Mexico.

Hassiotis, S., Jeong G.D. (1993): Assessment of Structural damage from natural frequency measurements, *Computers and Structures*, 49, 4, 679-691.

Hassiotis, S. (2000): Identification of damage us-

ing natural frequencies and Markov parameters, *Computers and Structures*, 74, 365-373.

Iacono, C., Sluys, L.J., Van Mier, J.G.M. (2006): Estimation of model parameters in non-local damage theories by inverse analysis techniques, *Compt. Methods Appl. Mech. Engrg.*, 195, 7211-7222.

Lakshmanan, N., Srinivasulu, P., Parameswaran V.S. (1991): Post cracking stiffness and damping in reinforced concrete beam elements, *Journal of Structural Engineering*, India, 17, 4, 1405-1411.

Lee, U., Cho, K., Shin, J. (2003): Identifica-

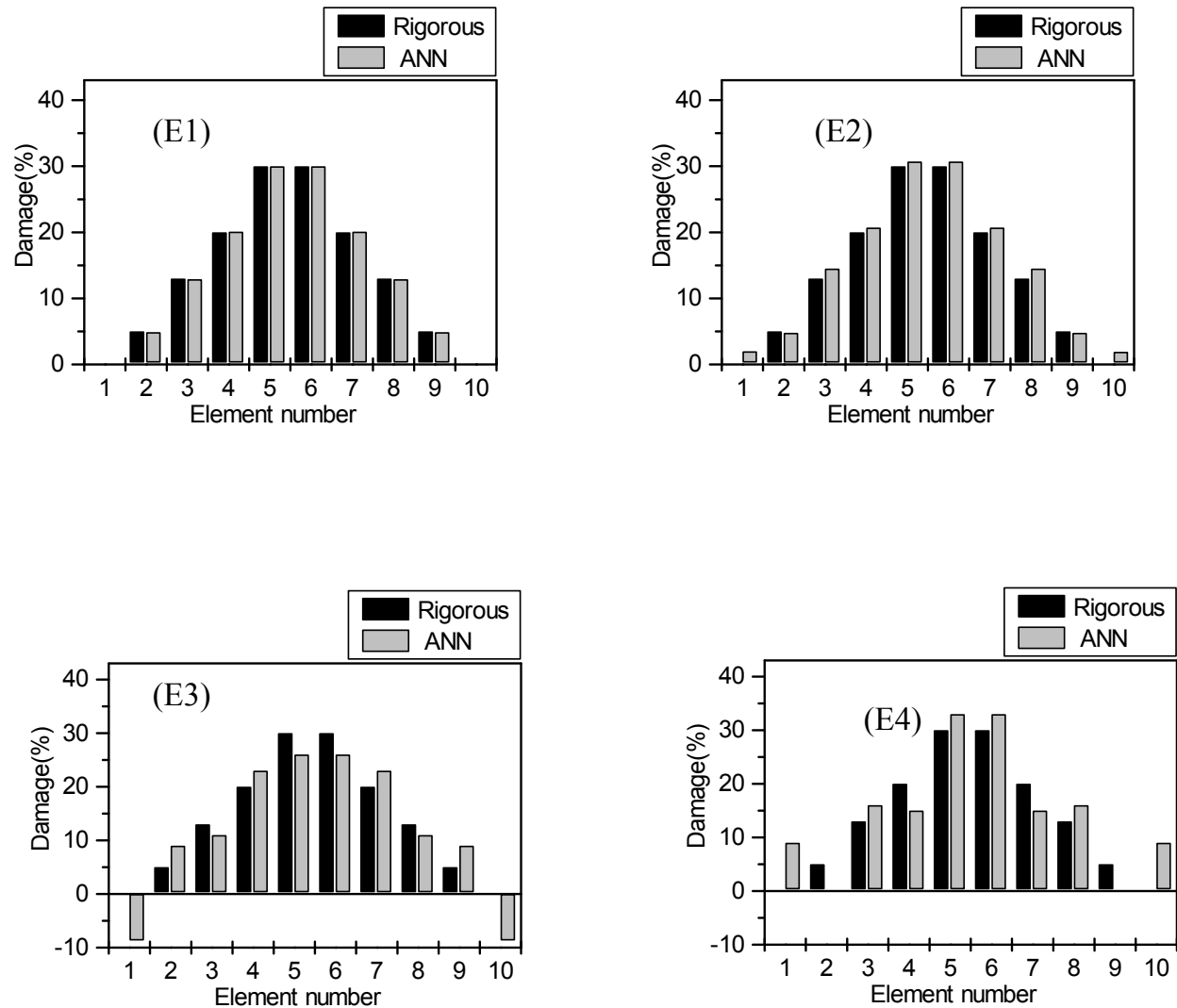


Figure 21: Performance Neural network under uniform (E1, E2) and fluctuating errors (E3, E4)

tion of orthotropic damages within a thin uniform plate, *Intl J. of Soilds and Structures*, 40, 2195-2213.

Li, Y.Y., Cheng L., Yam ,L.H., Wong, W.O. (2002): Identification of damage locations for plate-like structures using damage sensitive indices : strain modal approach, *Computers and Structures*, 80, 1881-1894.

Liu, J.K., Yang, Q.W. (2006): A new structural damage identification method, *Jl of Sound and Vibration*, 297, 694-703.

Ma Ge, Lui, E.M. (2005): Structural damage identification using system dynamic properties, *Computers and Structures*, 83, 2185-2196.

MATLAB-7, Mathworks Inc, Natick, MA.

Meo, M., Zumpano, G. (2005): Non-linear elastic wave spectroscopy identification of impact damage on a sandwich plate, *Composite structures*, 71, 469-474.

Morassi, A. (2007): Damage detection and generalised fourier coefficients, *Jl. of Sound and Vibration*, 302, 229-259.

Owolabi G.M., Swamidas, A.S.J., Seshadri R. (2003): Crack detection in beams using changes in frequencies and amplitudes of frequency response functions, *Journal of Sound and vibration*, 265, 1-22.

Rajagopalan, N., Lakshmanan, N., Muthu-

mani, K. (1996): Stiffness degradation of reinforced concrete beams under repeated low energy impact loading, *Indian Concrete Journal*, 69, 4, 227-234.

Rajagopalan, N., Lakshmanan, N., Jeyasehar C.A. (1999): Damage assessment in reinforced concrete beams using natural frequencies, *Journal of Structural Engineering*, India, 26, 3, 165-172.

Roy, S., Chakraborty, S., Sarkar, S.K. (2006): Damage detection of coupled bridge deck- girder system, *Finite Elements in Analysis and Design*, 42, 942-949.

Wu Di, Law, S.S. (2007): Eigen-parameter decomposition of element matrices for structural damage detection, *Engineering Structures*, 29, 519-528.

Yam, L.H., Li, Y.Y., Wong, W.O. (2002): Sensitivity studies of parameters for damage detection of plate-like structures using static and dynamic approaches, *Engineering Structures*, 24, 1465-1475.

Yang X.F., Swamidias A.S.J and Seshadri R. (2001): Crack identification in vibrating beams using the energy-based method, *Journal of Sound and vibration*, 244(2), 339-357.

Yong Xia, Hong Hao (2003): Statistical damage identification of structures with frequency changes, *Jl. of Sound and Vibration*, 263, 853-870.

Yu, L., Cheng, L., Yam, L.H., Yan, Y.J. (2007): Application of Eigen value perturbation theory for detecting small structural damage using dynamic responses, *Composite Structures*, 78, 402-409.